

University of Groningen

## Metabolic Remodeling in the Pressure-Loaded Right Ventricle

Koop, Anne-Marie C.; Bossers, Guido P. L.; Ploegstra, Mark-Jan; Hagdorn, Quint A. J.; Berger, Rolf M. F.; Sillje, Herman H. W.; Bartelds, Beatrijs

*Published in:*  
Journal of the American Heart Association

*DOI:*  
[10.1161/JAHA.119.012086](https://doi.org/10.1161/JAHA.119.012086)

**IMPORTANT NOTE: You are advised to consult the publisher's version (publisher's PDF) if you wish to cite from it. Please check the document version below.**

*Document Version*  
Publisher's PDF, also known as Version of record

*Publication date:*  
2019

[Link to publication in University of Groningen/UMCG research database](#)

*Citation for published version (APA):*

Koop, A-M. C., Bossers, G. P. L., Ploegstra, M-J., Hagdorn, Q. A. J., Berger, R. M. F., Sillje, H. H. W., & Bartelds, B. (2019). Metabolic Remodeling in the Pressure-Loaded Right Ventricle: Shifts in Glucose and Fatty Acid Metabolism-A Systematic Review and Meta-Analysis. *Journal of the American Heart Association*, 8(21), [012086]. <https://doi.org/10.1161/JAHA.119.012086>

**Copyright**

Other than for strictly personal use, it is not permitted to download or to forward/distribute the text or part of it without the consent of the author(s) and/or copyright holder(s), unless the work is under an open content license (like Creative Commons).

**Take-down policy**

If you believe that this document breaches copyright please contact us providing details, and we will remove access to the work immediately and investigate your claim.

*Downloaded from the University of Groningen/UMCG research database (Pure): <http://www.rug.nl/research/portal>. For technical reasons the number of authors shown on this cover page is limited to 10 maximum.*

# Metabolic Remodeling in the Pressure-Loaded Right Ventricle: Shifts in Glucose and Fatty Acid Metabolism—A Systematic Review and Meta-Analysis

Anne-Marie C. Koop, MD; Guido P. L. Bossers, MD; Mark-Jan Ploegstra, MD, PhD; Quint A. J. Hagdorn, MD; Rolf M. F. Berger, MD, PhD; Herman H. W. Silljé, PhD; Beatrijs Bartelds, MD, PhD

**Background**—Right ventricular (RV) failure because of chronic pressure load is an important determinant of outcome in pulmonary hypertension. Progression towards RV failure is characterized by diastolic dysfunction, fibrosis and metabolic dysregulation. Metabolic modulation has been suggested as therapeutic option, yet, metabolic dysregulation may have various faces in different experimental models and disease severity. In this systematic review and meta-analysis, we aimed to identify metabolic changes in the pressure loaded RV and formulate recommendations required to optimize translation between animal models and human disease.

**Methods and Results**—Medline and EMBASE were searched to identify original studies describing cardiac metabolic variables in the pressure loaded RV. We identified mostly rat-models, inducing pressure load by hypoxia, Sugen-hypoxia, monocrotaline (MCT), pulmonary artery banding (PAB) or strain (fawn hooded rats, FHR), and human studies. Meta-analysis revealed increased Hedges' *g* (effect size) of the gene expression of GLUT1 and HK1 and glycolytic flux. The expression of MCAD was uniformly decreased. Mitochondrial respiratory capacity and fatty acid uptake varied considerably between studies, yet there was a model effect in carbohydrate respiratory capacity in MCT-rats.

**Conclusions**—This systematic review and meta-analysis on metabolic remodeling in the pressure-loaded RV showed a consistent increase in glucose uptake and glycolysis, strongly suggest a downregulation of beta-oxidation, and showed divergent and model-specific changes regarding fatty acid uptake and oxidative metabolism. To translate metabolic results from animal models to human disease, more extensive characterization, including function, and uniformity in methodology and studied variables, will be required. (*J Am Heart Assoc.* 2019;8:e012086. DOI: 10.1161/JAHA.119.012086.)

**Key Words:** heart failure • metabolism • myocardial biology • pulmonary hypertension • remodeling

Right ventricular (RV) function is an important predictor for clinical outcome in a variety of cardiac diseases.<sup>1–4</sup> In patients with pulmonary hypertension (PH), RV failure is

the main cause of death.<sup>2</sup> Development of RV failure because of sustained pressure load is characterized by progressive diastolic dysfunction, changes in fibrotic content, and metabolic remodeling.<sup>5–9</sup> The healthy adult myocardium primarily uses long-chain fatty acids as substrates, in contrast to the fetal heart, which uses primarily glucose and lactate.<sup>10–13</sup> Under stress, the heart switches to a so-called “fetal phenotype”, which includes a change in substrate utilization from oxidative metabolism towards glycolysis.<sup>12</sup> While these changes may have advantages (ie, better ratio of ATP production versus oxygen use), they may also have disadvantages (eg, increase of stimulation of inflammatory cascades via intermediaries). The RV under pressure may be especially susceptible to changes in substrate utilization because of its unique physiological properties.<sup>14</sup> The RV is a thin-walled crescent-shaped structure that under physiological conditions is coupled to low-resistance pulmonary circulation. Increased pressure load in the RV, prevalent in PH, congenital heart disease, and also in left ventricle (LV) failure, causes a relatively high

From the Department of Pediatric Cardiology, University Medical Center Groningen, Center for Congenital Heart Diseases, University of Groningen, The Netherlands (A.-M.C.K., G.P.L.B., M.J.P., Q.A.J.H., R.M.F.B., B.B.); Department of Cardiology, University Medical Center Groningen, University of Groningen, The Netherlands (H.H.W.S.).

Accompanying Data S1, Tables S1 through S5, Figures S1 through S4 are available at <https://www.ahajournals.org/doi/suppl/10.1161/JAHA.119.012086>

Beatrijs Bartelds is currently located at the Division of Pediatric Cardiology, Department of Pediatrics, Erasmus University Medical Center, Sophia Children's Hospital, Rotterdam, The Netherlands.

**Correspondence to:** Anne-Marie C. Koop, MD, Hanzeplein 1, CA41, Postbus 30.001, 9700 RB Groningen. E-mail: [a.c.koop@umcg.nl](mailto:a.c.koop@umcg.nl)

Received February 9, 2019; accepted September 4, 2019.

© 2019 The Authors. Published on behalf of the American Heart Association, Inc., by Wiley. This is an open access article under the terms of the Creative Commons Attribution-NonCommercial-NoDerivs License, which permits use and distribution in any medium, provided the original work is properly cited, the use is non-commercial and no modifications or adaptations are made.

## Clinical Perspective

### What Is New?

- This is the first systematic review and meta-analysis studying metabolic adaptation of the right ventricle in response to pressure overload and includes studies in both animal models and humans.
- In the pressure-loaded right ventricle, glucose uptake and glycolysis were shown to be increased, mediated by insulin-independent mechanisms irrespective of the model used.
- In contrast, changes in mitochondrial respiratory capacity were variable and depended on the animal model used.

### What Are the Clinical Implications?

- This study implies that in developing and testing future therapeutic options targeting metabolism of the pressure-loaded right ventricle, one should account for causative factors.
- To establish actual translation from experimental models to human disease, experimental methods and outcome parameters should be standardized and uniform.

load for the RV. In addition, the RV may be more susceptible compared with the LV because of the relatively higher disadvantageous changes in coronary perfusion with increased afterload. Several studies have attempted to improve RV adaptation by metabolic modulation. Metabolic intervention tested whether direct or indirect stimulation of glucose oxidation by compounds such as dichloroacetate, ranolazine, trimetazidine, and 6-diazo-5-oxo-L-norleucine, could be supportive in the pressure-loaded RV.<sup>15–21</sup> Indeed, these modulations seem to affect cardiac performance positively, but because of the limited number of studies, different models, different compounds, and different study parameters, consensus has not been reached, complicating translation to clinical practice.<sup>22,23</sup> To support the validated setup of clinical trials and to identify challenges and opportunities in evaluating metabolic findings in animal models for human disease, a comprehensive appreciation of all evidence collected in previous studies addressing metabolic adaptation of the RV to pressure load is necessary. The aim of this systematic review and meta-analysis is to provide an overview of the current knowledge about metabolic remodeling, focusing on carbohydrate and fatty acid metabolism in the pressure-loaded RV. Both experimental and clinical studies were included, taking into account the different models or type of disease, and the degree and duration of RV pressure load, and RV- and clinical function. In addition, we present an overview of the studies performed regarding interventions affecting metabolism in the RV under pressure.

## Materials and Methods

The data that support the findings of this study are available from the corresponding author upon reasonable request.

### Literature Search

We performed a systematic literature search in Medline and EMBASE on November 29, 2017. The search strategy and global methodological approach using *Systematic Review Protocol for Animal Studies, version 2.0* formatted by SYRCLE<sup>24,25</sup> was published on the online platform of the working group Collaborative Approach to Meta-Analysis and Review of Animal Data for Experimental Studies (CAMARADES) on December 13, 2016. The search strategy was composed to capture overlapping parts of the following domains: (1) RV; (2) pressure load; and (3) metabolism (Data S1).

### Study Selection

Two researchers (A.M.C.K. and G.P.L.B.) independently screened the identified abstracts according to the following inclusion criteria: (1) English; (2) original article; (3) RV pressure load; (4) no reversible pressure load; (5) no mixed loading; and (6) RV metabolism. Full texts were screened for control group and sufficiency of the model by confirming increased pressure load by at least (1) increased RV pressure load (ie, RV systolic pressure or mean pulmonary artery pressure), or (2) hypertrophy (ie, RV weight, Fulton index (RV divided by LV+interventricular septum) or RV to body weight ratio). For inclusion of human studies, a control group for pressure load measurements was not required, since inclusion of individuals at study level did meet the criteria of international guidelines for pulmonary hypertension.<sup>26</sup>

### Data Extraction

For the meta-analysis inclusion, the study had to report on metabolic variables, which were investigated in at least 2 or more other studies. Variable of metabolism was defined as (1) mRNA expression of genes involved in substrate uptake of metabolism; (2) protein expression and/or activity of genes involved in substrate uptake of metabolism; or (3) metabolism measured in vivo or in vitro using either oxygraphy in isolated mitochondria (eg, Oroboros, Clark-type electrode), oxygraphy in whole cells (eg, Seahorse) or in isolated hearts (eg, Langendorf). General upstream regulators also involved in metabolism (eg, mitogen-activated protein kinase and AKT [protein kinase B]) were not included. In addition, study characteristics such as species, model/type of pressure load, and degree and duration of pressure load of selected studies were extracted. We extracted the mean, SD (if not presented,

SE), and number of subjects (n) of the selected variables from all eligible studies. Universal Desktop Ruler (Avpsoft) was used to derive data from graphs. In case of missing information, authors were contacted. If response was lacking, we approached the data as follows: when the SD was unknown, the SD was calculated when mean difference, (corrected) *P* value, and number of used subjects were available; in case of unknown SD of the control groups, we used the SD of the experimental group; if the exact n was unknown, the greatest number given was used for the calculation of the SD.

## Data Synthesis

Effect sizes, defined as Hedges' *g*, with associated CI of 95% were calculated, after which multiple separate random effects meta-analyses were performed using STATA 11. When the actual number of animals (n) used for a certain variable was unknown (ie, not reported in the manuscript and not acquired after contacting the author), the smallest n mentioned by the authors was used to calculate the Hedges' *g*. Combined effect sizes of a particular variable were calculated for (1) the different models (shown by the gray squares) and (2) all studies describing the variable (shown by the black squares). Heterogeneity was assessed using Cochran's Q-test and the  $i^2$  quantity. In order to explore the sources of heterogeneity, meta-regression analyses were performed for duration and degree of pressure load if information was available for more than 2 groups. To perform meta-regression analysis of a variable with duration, actual duration of pressure load had to be given (ie, variables were excluded from meta-regression analysis if corresponding duration was defined as a time-interval [eg, 2–6 weeks]). To be included for meta-regression analyses concerning the degree of pressure load, RV loading had to be measured as actual pressure rather than increase in hypertrophy. Unfortunately, meta-regression of cardiac or RV function was impossible because of lack of available data. In addition, differences between models were tested with unpaired *t* test or 1-way analysis of variance with post-hoc Tukey's correction.

Since they have different functions in biological processes, gene expression (at mRNA level) and protein expression of studied variables were separately included in the meta-analysis. In some studies, mitochondrial content was tested by different measurement techniques within the same animals. To avoid overrepresentation of included subjects, the results of only 1 (the superior) technique/definition was included for meta-analysis. We ranked the different definitions of mitochondrial content (which were used in the same animals) as follows: (1) ratio mitochondria to myofibrils, (2) mitochondrial yield, (3) citrate synthase activity, (4) citrate synthase at mRNA level, and (5) whole tissue citrate synthase

activity. However, all results (from all different techniques) are visually shown in the figures.

If the study concerned did not provide the exact number of animals used for the test of a particular variable, the mean of the range of the number of animals reported in the concerning study was presented in our figures.

The number of included animals per model provided in the current figures may give a slight overestimation in case of multiple groups using the same control group.

## Results

### Identified Studies

In total, 1393 unique citations were identified, as shown in Figure 1. Based on title abstract screening, 1282 citations were excluded. Of the 111 articles selected for full text review, 86 articles concerned animal studies and 28 articles concerned human studies, and 3 articles described both (Table S1). After full text review, 35 studies were excluded because no control group for the metabolic variables was included (n=22), no increase in RV pressure was measured (n=11), or full text was not available (n=2). The former involved mostly the human studies. We included 28 studies for meta-analysis (Table S1); 2 of the studies described both human and animal data (Piao, 2013<sup>16</sup> and Gomez-Arroyo, 2013<sup>27</sup>).

From 3 selected publications, 3 study groups were excluded (Balestra 2015, MCT30<sup>28</sup>; Rumsey 1999, 1 day<sup>29</sup>; and Zhang 2014, 2 weeks<sup>30</sup>), since pressure load and hypertrophy did not increase significantly or was not reported. All other groups had at least increased RV systolic pressure (Figure S1A), RV weight, Fulton index (Figure S1B), or RV/body weight ratio.

### Glucose Transport and Glycolysis

We identified 3 variables of glucose transport that were described in 3 or more studies: fluorodeoxyglucose (FDG) uptake and expression of transporters GLUT1 and 4 (Figure 2). The uptake of the glucose-analogue FDG was uniformly increased in animal models<sup>19,31,32</sup> as well as in patients with PH<sup>33</sup> (Figure 2A). Numerous studies investigated the expression of the major glucose transporters, GLUT1 and GLUT4, and correlated this with FDG uptake. Our meta-analysis revealed that GLUT1 mRNA as well as protein level were significantly increased in the pressure-loaded RV (Figure 2B). The increase in GLUT1 mRNA expression was universal in all models,<sup>15,18,21,27,34–37</sup> but protein levels were higher in the monocrotaline (MCT) model<sup>15</sup> as compared with the hypoxia, pulmonary artery banding (PAB), and fawn hooded rat (FHR) models<sup>15,16,21</sup> ( $P<0.05$  for all groups). In

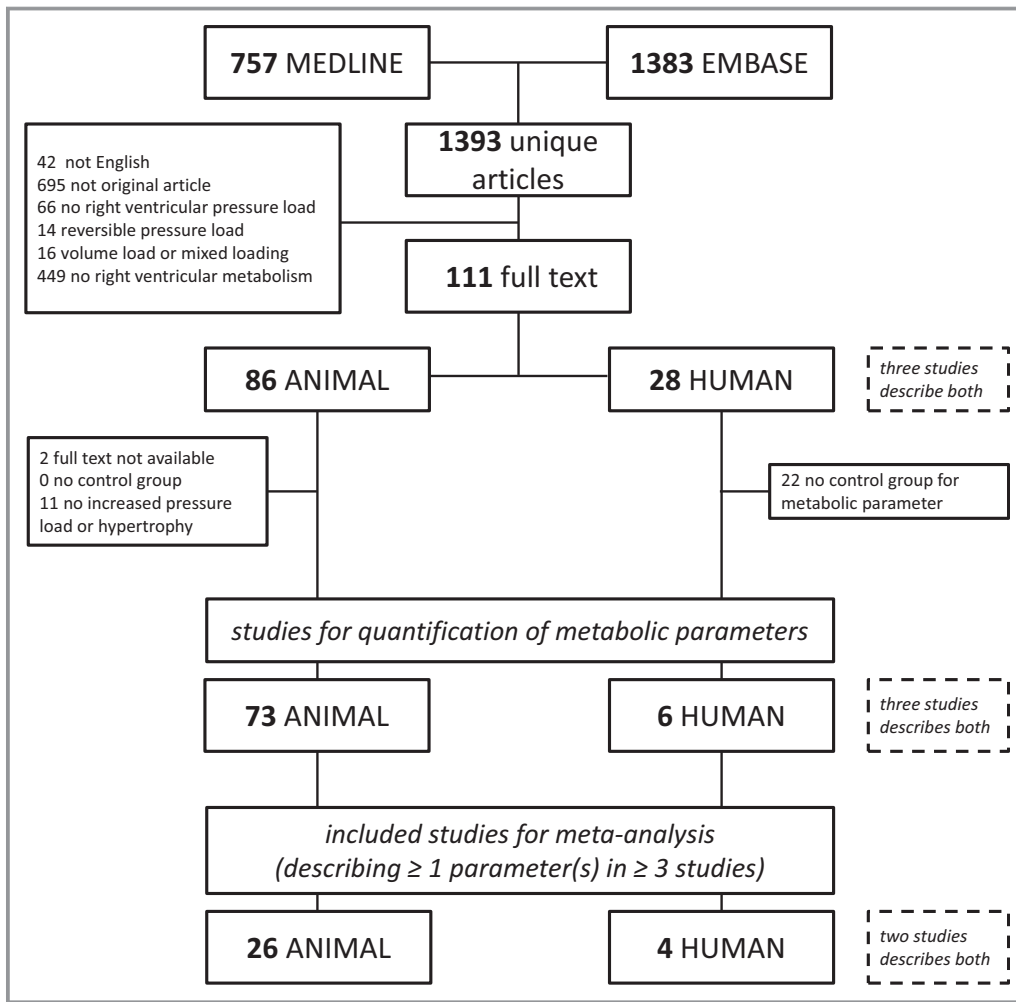


**Figure 1.** Flow chart of systematic study selection and inclusion meta-analysis.

contrast to GLUT1, the gene expression of GLUT4<sup>34–36</sup> and the GLUT4 proteins levels<sup>19,36,38–40</sup> were not altered (Figure 2C). Meta-regression analyses for FDG-uptake, GLUT1 and GLUT4, revealed no statistical significant correlations with duration or degree of RV pressure load (Table S2). Meta-regression of GLUT1 at protein level and GLUT4 at gene level with degree of RV pressure load is not performed because of missing pressure measurements in the studies concerned.

Glucose transport is coupled with glucose-phosphorylation by hexokinases, driving glucose into glycolysis. The mRNA expression of HK1 (Figure 3A) was significantly increased in all models.<sup>18,21,27,29,30</sup> In addition, meta-regression analysis showed a negative trend with the duration of RV pressure load ( $P=0.08$ ) (Figure 3B). HK2 expression was not altered<sup>15,16,21,27,29,30,37</sup> (Figure 3C) and meta-regression analysis revealed no correlations with duration of degree of pressure load (Tables S2 and S3). Unfortunately, protein levels of HK1 were only determined in 1 study<sup>18</sup> and HK2 protein levels were not determined at all, and therefore it is unclear how HK protein levels are affected by

pressure overload. Glycolysis was studied on isolated hearts in a Langendorf perfusion system of 3 RV pressure overload models: MCT,<sup>15</sup> PAB,<sup>21</sup> and FHR.<sup>16</sup> In addition, glycolysis was determined by Seahorse in RV preparations of the FHR model.<sup>16</sup> Meta-analysis of the data revealed that glycolysis was significantly increased in cardiac tissue of these RV pressure-loaded hearts (Figure 3D).

### Transport of Fatty Acids

Transporter cluster differentiation 36 (CD36), the main transporter of fatty acids across the plasma membrane, was only investigated in 3 studies (either RNA or protein)<sup>27,37,41</sup> and hence did not meet the criteria for meta-analysis. Transport of fatty acids over the mitochondrial membrane is highly regulated by carnitine palmitoyltransferases (CPT1 and CPT2) (outer and inner membrane, respectively). Only meta-analysis of subunit CPT1B was possible, but revealed ambiguous and nonsignificant results<sup>16,27,34,37</sup> (Figure 4A).

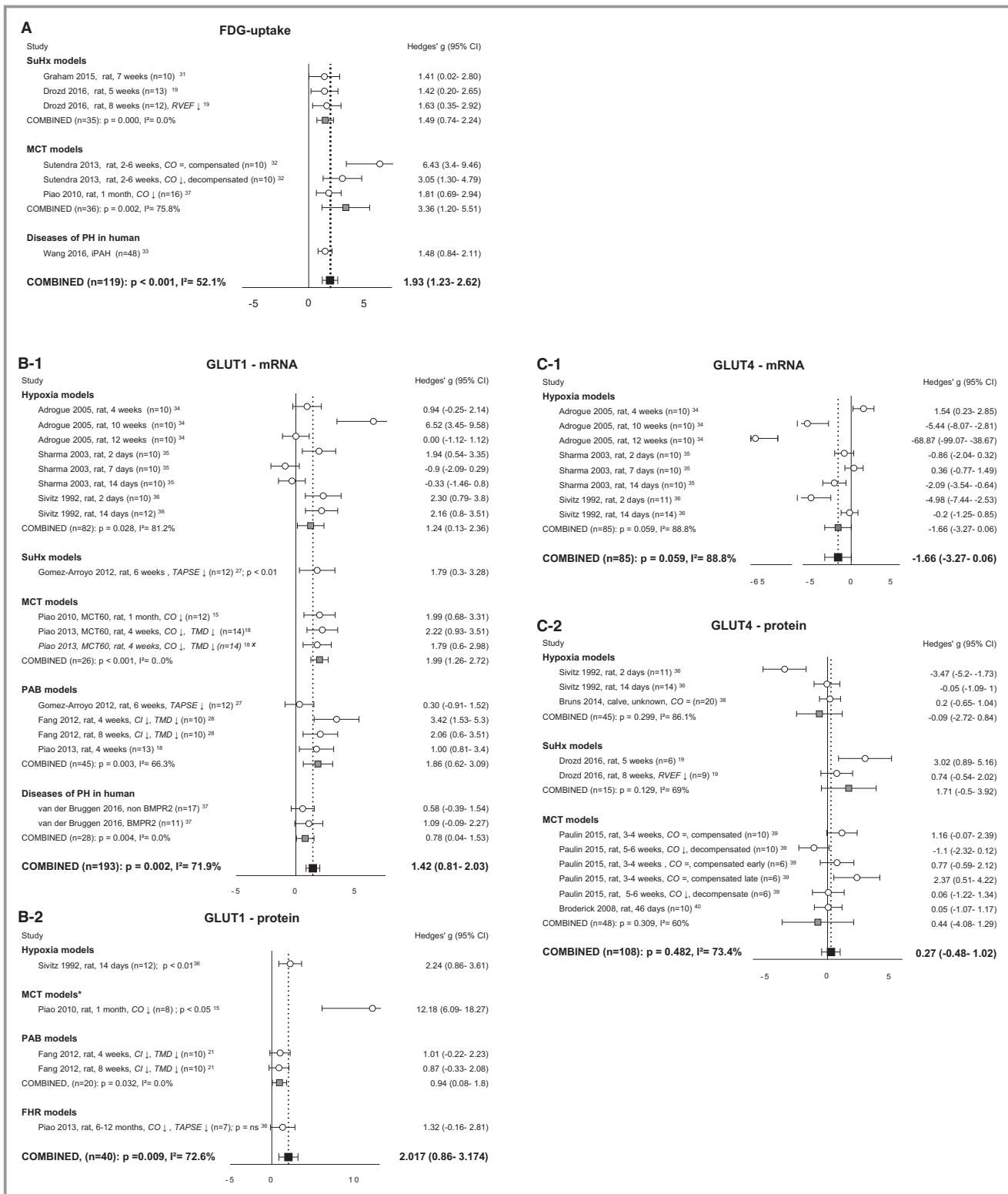


**Figure 2.** Right ventricular uptake of carbohydrates. Forrest plots of FDG-uptake (A), GLUT1 expression at mRNA (B-1) and protein (B-2) level, and GLUT4 expression at mRNA (C-1) and protein (C-2) level. Data are presented as Hedges' g. Combined Hedges' g are presented as squares: gray representing Hedges' g of a specific model, black representing Hedges' g of all included studies. Bars represent 95% CI. = indicates not statistically significant affected; ↓, decreased; CI, cardiac index; CO, cardiac output; FDG uptake, fluorodeoxyglucose uptake; GLUT, glucose transporter; i<sup>2</sup>, level of heterogeneity; MCT, monocrotaline; n, number of included animals; RVEF, right ventricular ejection fraction; TAPSE, tricuspid annular plane systolic movement; X, not included in meta-analysis. \*Significantly (P<0.05) increased compared with hypoxia, pulmonary artery banding- and fawn hooded rats-models.

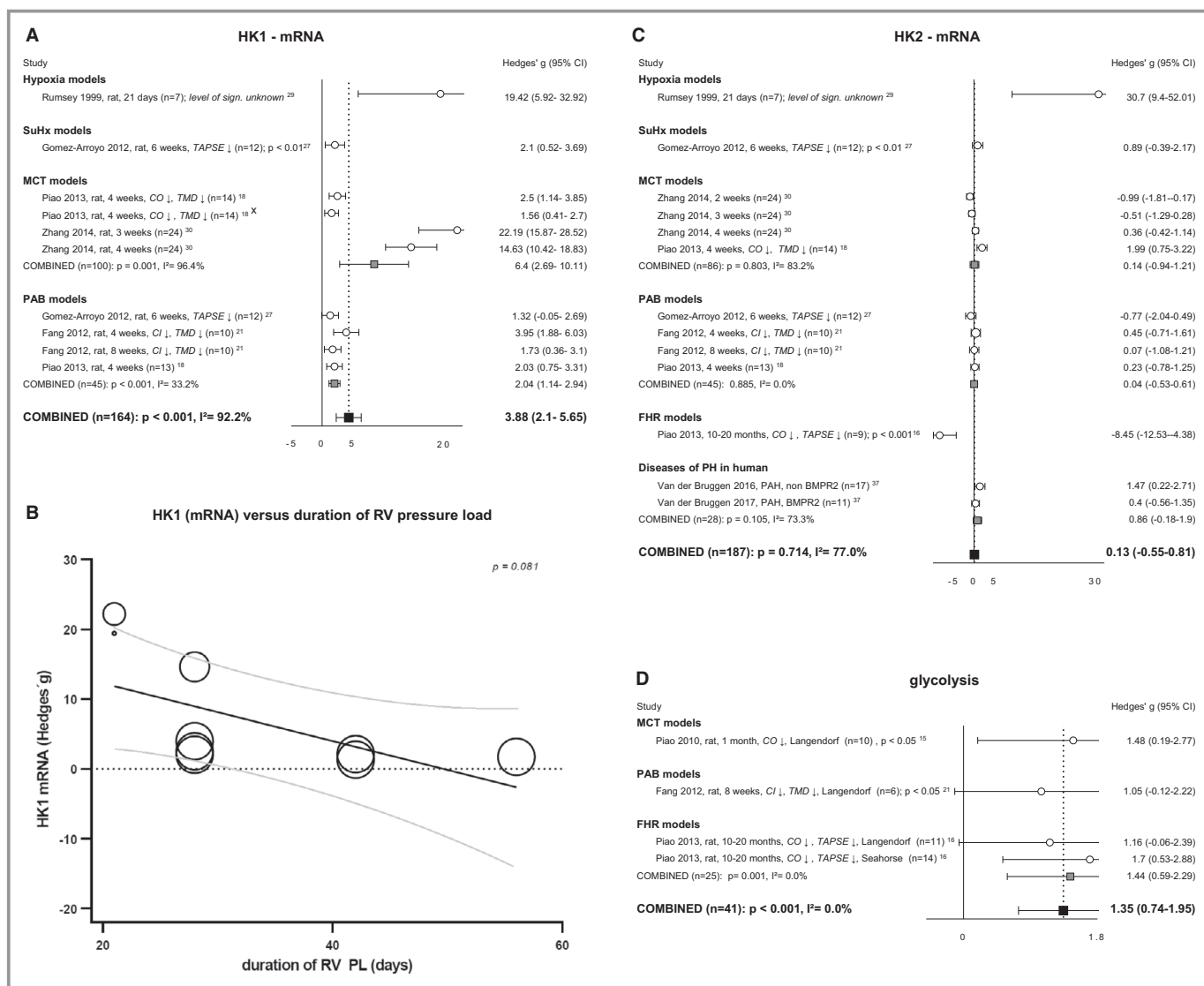


**Figure 3.** Glycolysis. Forrest plot of HK1 (A) and bubble plot showing meta-regression analysis of HK1 expression at mRNA level with the duration of RV pressure load (B). Forrest plots of HK2 (C) expression at mRNA level and glycolytic flux measured with Seahorse or Langendorf (D). Data are presented as Hedges' g. Combined Hedges' g are presented as squares: gray representing Hedges' g of a specific model, black representing Hedges' g of all included studies. Bars represent 95% CI. Bubble size represents relative study precision, calculation based on SD. Black line represents regression line, gray lines represents 95% CI. = indicates not statistically significantly affected; ↓, decreased; 95% CI, cardiac index; CO, cardiac output; FHR, fawn hooded rats; HK, hexokinase; I<sup>2</sup>, level of heterogeneity; MCT, ; n, number of included animals; PAB, pulmonary artery banding; PH, pulmonary hypertension; RVEF, right ventricular ejection fraction; TAPSE, tricuspid annular plane systolic movement; X, not included in meta-analysis.

However, CPT1B mRNA negatively correlated with duration of pressure overload (Figure 4B).

## Mitochondrial Function

### Mitochondrial content

Mitochondrial content was studied using different assays and was subsequently expressed as the following: the ratio of mitochondrial DNA – nuclear (18S) DNA, the ratio of the number of mitochondria to myofibrils, mitochondrial yield (mg

mitochondrial protein per gram RV), and citrate synthase activity or citrate synthase mRNA expression. Combining all the data from different models<sup>27,28,42–45</sup> and including all analyses, a significant decrease of mitochondrial content in the pressure-loaded RV could be demonstrated ( $g = -0.60$ ,  $P = 0.016$ ). However, several studies used data from the same experiment. After exclusion of the possible duplicate measurements (choosing most optimal determination, ranked according to order above), mitochondrial content tended to decrease, but lost its statistical significance ( $g = -0.68$ ,

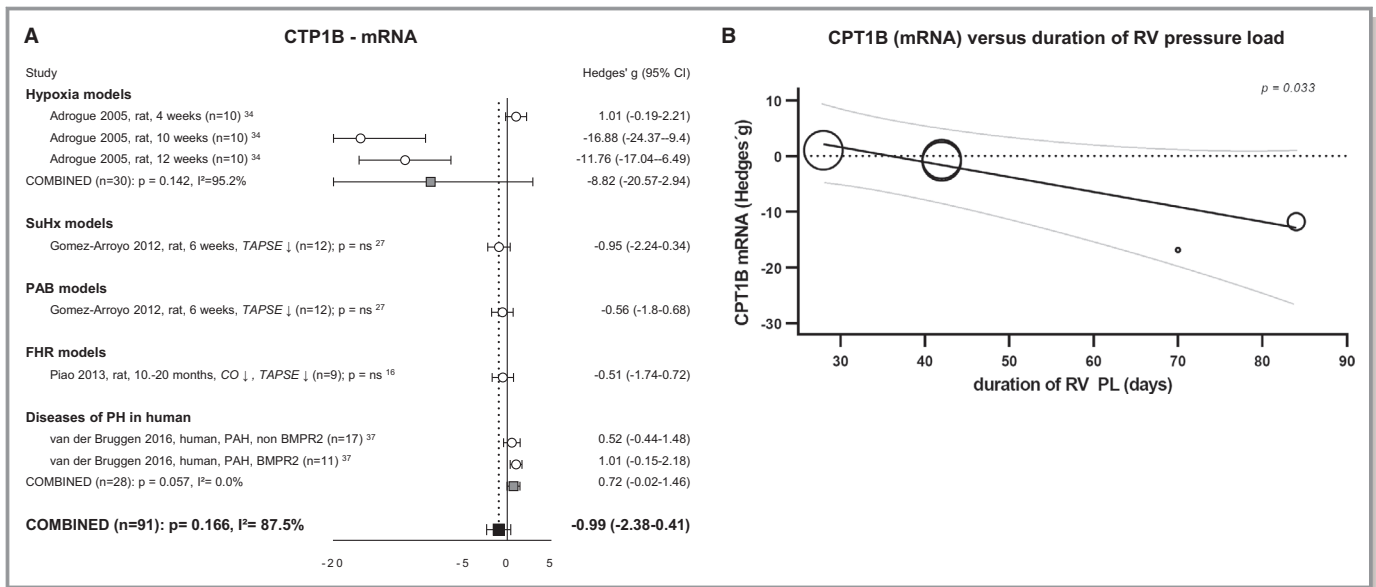


**Figure 4.** Right ventricular uptake of fatty acids. Forrest plot of CPT1B expression at mRNA level (A). Bubble plot showing the relation between CPT1B expression at mRNA level with duration of pressure load (B). Data are presented as Hedges' g. Combined Hedges' g are presented as squares: gray representing Hedges' g of a specific model, black representing Hedges' g of all included studies. Bars represent 95% CI. Bubble size represents relative study precision, calculation based on SD. Black line represents regression line, gray lines represents 95% CI. = indicates not statistically significant affected; ↓, decreased; CI, cardiac index; CO, cardiac output; CPT1B, carnitine palmitoyltransferase; FHR, fawn hooded rats; I<sup>2</sup>, level of heterogeneity; n, number of included animals; PAB, pulmonary artery banding; PH, pulmonary hypertension; PL, pressure load; RV, right ventricular; TAPSE, tricuspid annular plane systolic movement.

$P=0.054$ ) (Figure 5A). Plotting duration against mitochondrial content suggests a curvilinear association, with a significant negative correlation in the first 6 weeks (Figure 5B). In addition, mitochondrial content is negatively correlated with the degree of RV pressure load (Figure S4).

### Glucose oxidation

Activity of pyruvate dehydrogenase (PDH), the enzyme converting pyruvate into acetyl-CoA in the mitochondria, tended to be decreased in RV pressure load but did not reach statistical significance ( $g=-1.982$ ,  $P=0.123$ )<sup>15,16,18,21</sup> (Figure 5C). A similar result was observed for PDK4, a negative regulator of PDH, (resp.  $g=-1.91$ ,  $P=0.110$ ), where meta-analysis of expression at both mRNA<sup>16,34,35</sup> and protein level<sup>16,17,32</sup> was unchanged (Figure S2A, S2B). The same was true for PDK1 and PDK2 at protein level<sup>16,17,32</sup> (Figure S2C, S2D). Heterogeneity was not explained by the duration or degree of pressure load (Tables S2 and S3), or the different models.

Respiratory capacity of glucose or pyruvate was reported in 7 articles. Analysis was divided in ADP-driven respiratory state measured in isolated mitochondria with oxygraphy (Oroboros or Clark-type) ( $n=2$ )<sup>20,29</sup> (Figure 5D-1), and respiratory capacity measured in intact cardiomyocytes with Seahorse ( $n=2$ )<sup>16,21</sup> or isolated heart model (Langendorf) ( $n=3$ )<sup>15,16,18</sup> (Figure 5D-2). Subsequently, measurements in isolated mitochondria did not meet the inclusion criteria for meta-analysis. Respiratory capacity measured by all methods showed a

negative trend, albeit meta-analysis of respiratory capacity for carbohydrates in intact cardiomyocytes did not reveal a significant decrease ( $g=-1.21$   $P=0.082$ ). Respiratory capacity did increase in the MCT model compared with PAB ( $P<0.05$ ) (Figure 5D). Meta-regression analyses did not reveal correlations between respiratory capacity and duration or degree of RV pressure load.

### Oxidative fatty acid metabolism

β-Oxidation involved genes including ACADVL (1), EHHADH (2), HADHA (1), ACAA2 (3), ACAT1 (1), medium chain acyl CoA dehydrogenase (MCAD) (synonym ACADM) (6), ACADS (3), and ACOT2 (1) were all described, but only MCAD met the criteria for inclusion in meta-analysis. MCAD at the mRNA level decreased in all models of RV pressure load (hypoxia  $P<0.001$ , SuHx  $P<0.01$ , and PAB  $P<0.05$ )<sup>5,27,34,35,46</sup> (Figure 5E). No correlations with duration or degree of pressure load were observed (Tables S2 and S3). At the protein level, 3 studies<sup>27,46,47</sup> were included in the meta-analysis, which tended to decrease, but did not reach statistical significance ( $g=-2.02$ ,  $P=0.141$ ) (Figure S3).

Mitochondrial respiration regarding fatty acid oxidation measured in the ADP-driven state ( $n=4$ ) decreased, when tested in models of hypoxia<sup>29,42</sup> and SuHx<sup>20</sup> (Figure 5F-1). Respiratory capacity in intact cardiomyocytes was extracted from 2 publications showing contrary results in PAB<sup>21</sup> compared with the FHR model<sup>16</sup> (Figure 5F-2).



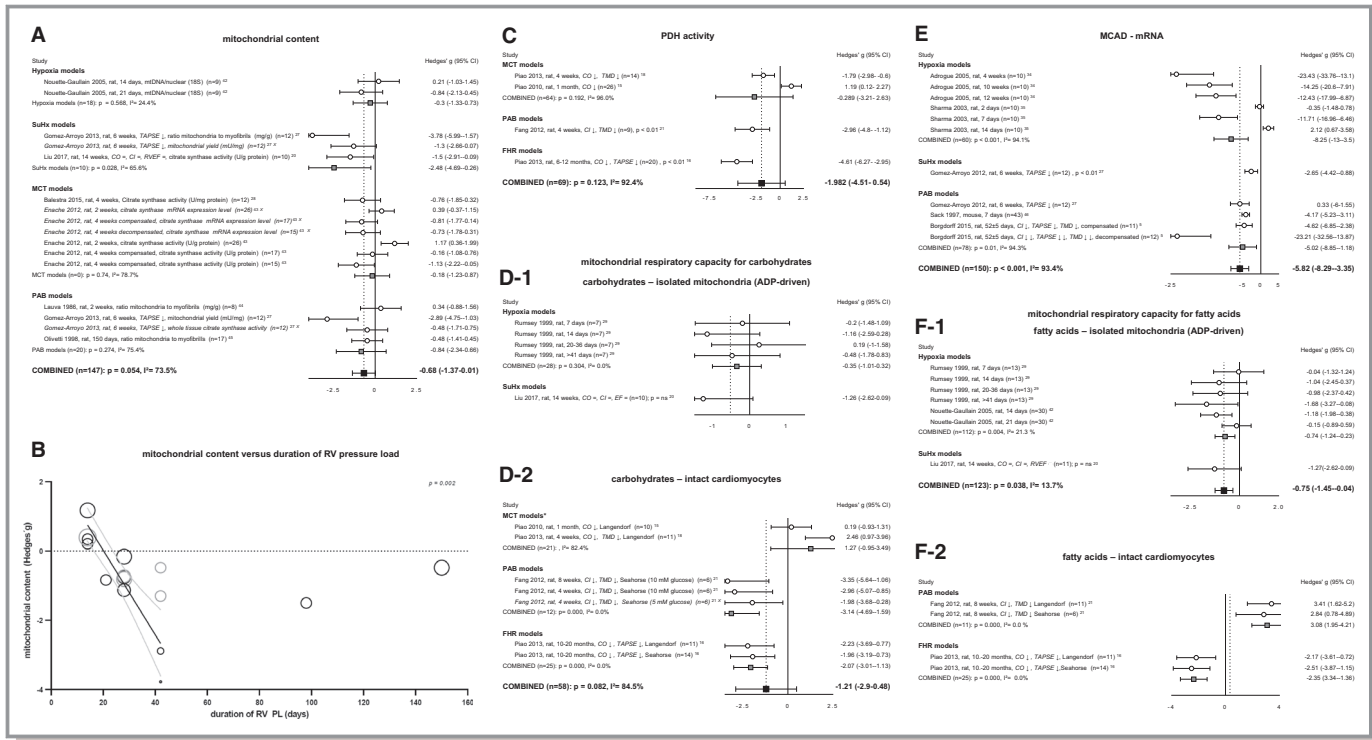


**Figure 5.** Mitochondrial function. Plots of mitochondrial content measured by mentioned methods (A). Bubble plot showing relation between mitochondrial content and duration of RV PL (B). Forrest plot of PDH activity as reflection of mitochondrial breakdown of pyruvate to acetyl-CoA (C). Forrest plots of mitochondrial respiratory capacity for carbohydrate metabolites measured in isolated mitochondria (ADP-driven) (D-1) or intact cardiomyocytes (D-2). Forrest plots of MCAD expression at mRNA level (E), as representative of the  $\beta$ -oxidation. Forrest plots of mitochondrial respiratory capacity for fatty acids measured in isolated mitochondria (F-1) and intact cardiomyocytes (F-2). Data are presented as Hedges' g. Combined Hedges' g are presented as squares: gray representing Hedges' g of a specific model, black representing Hedges' g of all included studies. Bars represent 95% CI. Bubble size represents relative study precision, calculation based on SD. Gray bubbles are not included in meta-analysis. Black line represents regression line, gray lines represent 95% CI.  $\downarrow$ , decreased;  $\downarrow\downarrow$ , decreased compared with decompensated group; CI, cardiac index; CO, cardiac output; FHR, fawn hooded rats;  $I^2$ , level of heterogeneity; MCT, monocrotaline; n, number of included animals; PAB, pulmonary artery banding; PDH, pyruvate dehydrogenase; PL, pressure load; RVEF, RV ejection fraction; TAPSE, tricuspid annular plane systolic movement; X, not included in meta-analysis. \*Significantly ( $P < 0.05$ ) increased compared with PAB.

**Transcriptional Regulators of Metabolism**

This systematic search identified several regulators of transcriptional regulators of metabolism (ie, PGC1 $\alpha$  (5), PPAR $\alpha$  (4), PPAR $\gamma$  (1), FOXO1 (1), Mef2c (1), HIF1 $\alpha$  (4), and cMyc (1)) (numbers include both gene expression at mRNA level and protein expression). Meta-analysis was performed for PGC1 $\alpha$  and PPAR $\alpha$ . PGC1 $\alpha$  is best known as the master regulator of mitochondrial biogenesis and interacts with PPAR $\alpha$ , which predominantly acts on lipid metabolism. Combined Hedges' g of PGC1 $\alpha$  mRNA expression<sup>27,43</sup> decreased (Figure S4B) and meta-regression revealed a negative correlation with duration of pressure load (Figure S4C). Meta-analysis for PGC1 $\alpha$  protein expression did not reveal significant change (Figure S4D), but did show a model effect for MCT<sup>43</sup> versus SuHx<sup>20,27</sup> ( $P < 0.05$ ) (Figure S4B). Combined Hedges' g of PPAR $\alpha$  mRNA expression<sup>27,34,35</sup> during pressure load did not change significantly (Figure S4E) and no correlations with

duration, degree, or model of RV pressure were observed. PPAR $\alpha$  protein expression was studied once in SuHx rats, demonstrating a decrease ( $P < 0.001$ ).<sup>27</sup>

Results are summarized in Figure 6 and Table S4.

**Effect of Interventions on Metabolism in the Pressure-Loaded RV**

Twenty studies described the effect of an intervention on metabolic parameter(s). Overall, these intervention studies aimed to decrease glycolysis by the increase of glucose oxidation. This could be established by recoupling of glycolysis with glucose oxidation, by, for example, dichloroacetate or 6-diazo-5-oxo-L-norleucine, or indirectly by inhibition of fatty acid metabolism by, for example, trimetazidine or ranolazine. Seven studies included metabolic variables that were included in meta-analyses above.<sup>15-21</sup> Of these metabolic variables, effect sizes derived from certain metabolic

Downloaded from http://ahajournals.org by on December 17, 2019

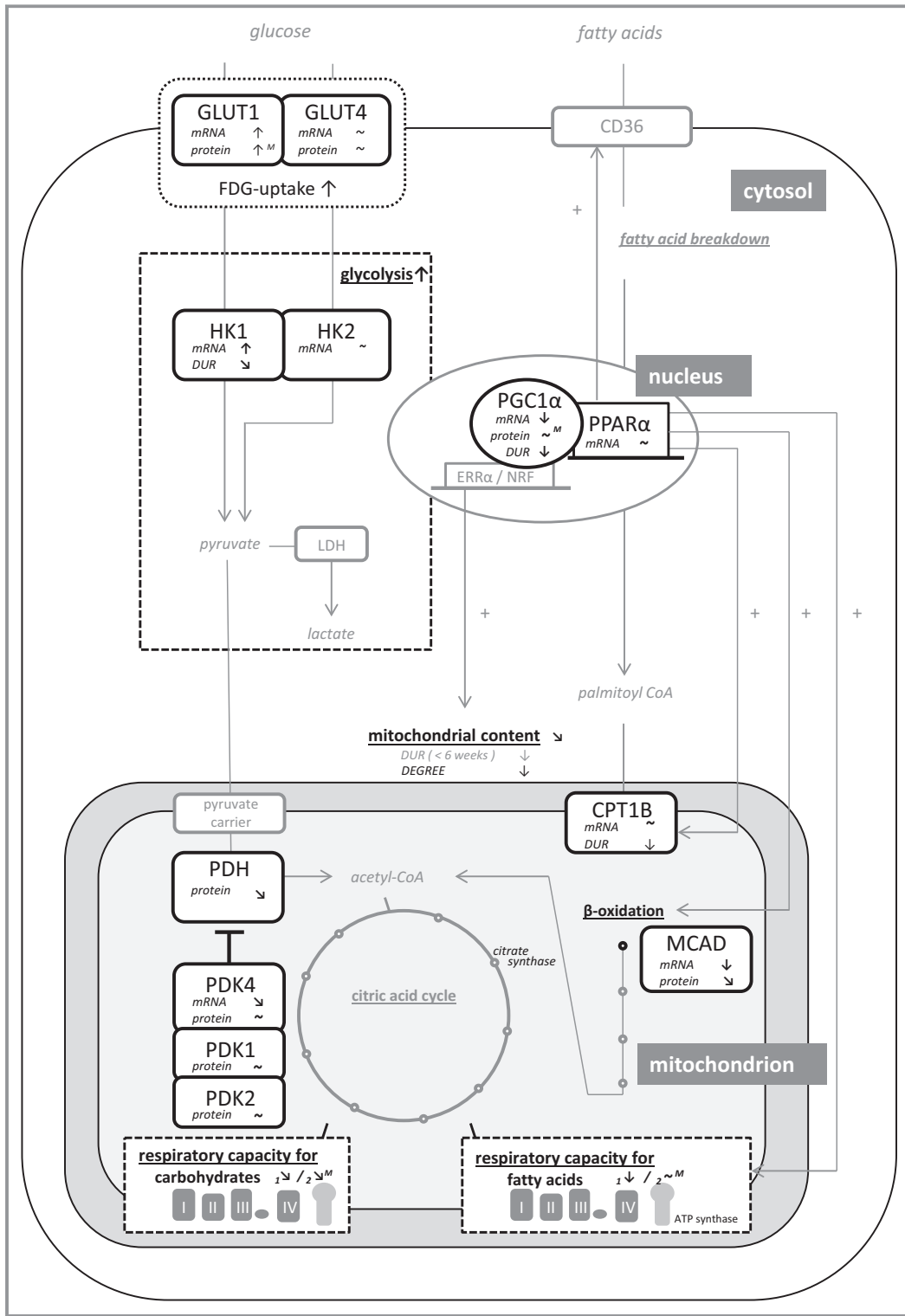


**Figure 6.** Metabolic changes in the pressure-loaded right ventricle: summarizing results of multiple meta-analyses. Black components are included in meta-analysis. ~ indicates unchanged; ↑, significant increase or positive relation; ↗, positive trend ( $P < 0.15$ ); ↘, negative trend ( $P < 0.15$ ); ↓, significant decrease or negative relation; CD36, cluster differentiation 36 (cellular fat transporter); CPT1B, carnitine palmitoyltransferase 1B; DUR, duration; ERRα, estrogen-related receptor alpha; FDG-uptake, fluorodeoxyglucose uptake; GLUT, glucose transporter; HK, hexokinase; LDH, lactate dehydrogenase; *M*, model effect; MCAD, medium chain acyl CoA dehydrogenase; NRF, nuclear respiratory factor; PDH, pyruvate dehydrogenase; PDK, pyruvate dehydrogenase kinase; PGC1α, PPAR gamma complex 1 alpha; PPARα, peroxisome proliferator-activated receptor alpha.

variables of the intervention group treated with metabolic therapy compared with those of the intervention group without treatment are shown in Table S5. The effect of dichloroacetate on PDH activity was studied in 3 studies showing a significant increase in a FHR model,<sup>16</sup> with contrary results regarding 2 MCT models.<sup>15,17</sup> The effects of therapeutic interventions on all other 21 reported variables were studied incidentally, precluding data synthesis and conclusions.

## Discussion

In this systematic review on metabolism in the pressure-loaded RV, we identified 26 animal and 4 human studies eligible for meta-analysis. The systematic review combined with multiple separate meta-analyses yielded a uniform increase in glucose uptake and glycolysis, whereas fatty acid uptake and changes in oxidative metabolism were less consistent. The effect of therapeutic interventions could not be analyzed because of the large variety of outcome variables used and compounds used.

In the current study, there are strong indications that glycolysis is increased in the pressure-overloaded RV. Both gene expression of HK1, an important enzyme controlling the first step of glycolysis, and the capacity for glycolysis measured by Seahorse and Langendorf were significantly increased. In contrast, HK2 was unchanged. Previous studies in the LV have identified HK2 as a modulator of reactive oxygen species and described attenuating effects on cardiac hypertrophy.<sup>48,49</sup> HK2, involved in anabolic pathways by providing glucose-6-phosphate for glycogen synthesis, also fulfills a role in providing glucose-6-phosphate to the pentose phosphate pathway. Contrary to the many roles of HK2, HK1 primarily facilitates glycolysis.<sup>50,51</sup> HK1 is primarily expressed in neonatal cardiomyocytes and is associated with the fetal gene program,<sup>50,52,53</sup> characterized by better resistance against an oxygen-poor environment such as in the RV pressure load.<sup>5,39,54–56</sup> The activation of the fetal gene program is also reflected in an increased expression of GLUT1, supporting increased glucose uptake, which increases the ability of increased glycolysis.<sup>16,27,32</sup> Remarkably, HK1 and GLUT1 both concern insulin-independent isoforms whereas HK2 and GLUT4 concern insulin-dependent isoforms.<sup>57</sup> The current meta-analysis reveals a clear pattern in the pressure-overloaded RV differentiating between the insulin-independent versus insulin-dependent profiles, directing to glycolysis by activation of insulin-insensitive mechanisms.

The increase of glycolysis in the pressure-loaded RV is also supported by the increased glucose uptake measured by FDG by positron emission tomography (PET)-computed tomography. PET-computed tomography has the ability to assess the

actual uptake in vivo, whereas gene or protein expression of involved genes and respiratory capacity of isolated mitochondria are an approximation of the actual situation in vivo. However, FDG uptake represents glucose uptake rather than metabolic capacity itself. Studies describing FDG uptake that were excluded from meta-analysis endorse our findings.<sup>58–62</sup> In addition, increased RV FDG uptake has been associated with increased pressure load<sup>58,60,63,64</sup> and altered dimensions,<sup>60,62,64,65</sup> and inverse correlations with RV function,<sup>62,63,65</sup> cardiac function,<sup>60</sup> and clinical outcome.<sup>66,67</sup>

Meta-analysis of substrate-specific oxidative metabolism in the pressure-loaded RV reflects an ambiguous character. Glucose oxidation is regulated via pyruvate dehydrogenase kinase, which inhibits breakdown of pyruvate. The expression of pyruvate dehydrogenase kinase in response to pressure load in the RV varied widely with different models used (Figure S4A through S4D). In addition, the respiratory capacity for carbohydrates was also affected by the model used. Although cardiac performance was decreased in both MCT and PAB models to the same extent, respiratory capacity increased in MCT models, but decreased in pressure load only via PAB. Similarly, with respect to respiratory capacity for fatty acids, PAB models behaved differently from FHR, while there are no data from MCT models. Taken together, these data suggest that the RV oxidative capacity changes in response to pressure load are dependent upon methodological differences, and may be subsequently dependent on model or disease, cardiac function, and possibly on clinical severity. More cooperation between research groups and comparative studies between fixed RV-PA uncoupling (in PAB) versus dynamic RV-PA uncoupling (eg, in MCT) are needed to identify the systemic changes that may interfere with the cardiac response. Intriguingly, whereas there was variation in the respiratory capacity for fatty acids, the changes in 1 of the genes oxidizing fatty acids (MCAD) were uniform. Downregulation of the  $\beta$ -oxidation was supported in the literature by decrease of other genes from the acyl-coenzyme A (CoA) dehydrogenases family at both mRNA<sup>16,27</sup> and protein level.<sup>27,46,68</sup> Downregulation of the oxidation phase has been suggested based on decreased expression of genes as HADH,<sup>5,69</sup> HADHA, HADHB, and EHHADH.<sup>5,68,70</sup> In addition, malonyl-CoA decarboxylase is described to be decreased in a model of hypoxia.<sup>34</sup> Oxidative metabolism in general in the pressure-loaded RV was studied in 2 studies and therefore is not included in the meta-analysis. The clearance of <sup>11</sup>C-acetate was used as representative of the tricarboxylic cycle. RV clearance rates correlated with the rate pressure product and oxygen consumption in idiopathic pulmonary arterial hypertension (iPAH),<sup>71</sup> and appeared to be higher PH (chronic thromboembolic PH [CTEPH], pulmonary arterial hypertension (PAH), and PH with unclear multifactorial mechanisms) compared with controls.<sup>72</sup> The current study stresses the

need for further research in order to clarify changes caused by pressure load itself and changes as a result of the specific inducement of RV pressure load or a potential systemic disease.

The systematic literature search showed that processes involved in the transport of long-chain fatty acids varied in different models and different cohorts of patients with PH. Gene expression of CD36, the transporter of long-chain fatty acids across the cellular membrane, was decreased in SuHx rats, unaffected in PAB rats, and increased at protein level in patients with a BMPR2 mutation.<sup>27,41</sup> Studies measuring gene expression of fatty acid binding proteins (FABP1-7) and fatty acids transporters (SLC7A1-6) in the pressure-loaded RV are scarce and were ambiguous.<sup>16,31</sup> We excluded studies describing actual fatty acid uptake measured with positron emission tomography tracers in the patient cohort without a control group. These studies also yielded various changes. Different cohorts representing different types of diseases, including precapillary PH and chronic obstructive lung disease, showed both pressure load-dependent<sup>73,74</sup> and –independent<sup>59,60,75</sup> cellular uptake. Support of load-dependent uptake was given by the reversibility of increased uptake after abolishing increased pressure load in patients with chronic thromboembolic PH.<sup>74</sup> In addition, positive correlations between fatty acid uptake and markers of RV hypertrophy were observed<sup>60,75</sup> and, as shown for glucose uptake measured by positron emission tomography–computed tomography, uptake of free fatty acids has been inversely correlated with RV ejection fraction<sup>59,75</sup> as well. Although no correlation was found with cardiac index,<sup>74</sup> fatty acid uptake has been positively correlated with clinical outcome, expressed by 6-minute walking distance, New York Heart Association class, and mortality.<sup>74,75</sup> Mitochondrial uptake of long-chain fatty acids in the healthy heart is predominately facilitated by CPT1B. CPT1B at the mRNA level negatively correlated with the duration of pressure load (Figure 4B). However, CPT1B expression in human forms of PAH tended to increase.<sup>37</sup> Few studies described CPT1A, describing inconsistent results.<sup>14,16,27,76</sup> Although CPT1A was originally considered an insignificant player in muscle (including heart) tissue, recent publications identified increased CPT1A as a key step in early metabolic remodeling, which is linked to reduced fatty acid oxidation.<sup>77</sup> Besides the contradictory results regarding fatty acid uptake between the different animal models and between different patient cohorts, no structural consistency was found between a specific animal model with a specific human disease. Nevertheless, a disease-specific pattern seems to apply for intramyocardial lipid deposition. Published results indicate lipid accumulation based on decreased fatty acid oxidation and increased fatty acid uptake by increased translation of CD36 to plasma membrane in heritable PAH specifically,<sup>78,79</sup> whereas RV

ceramide content in chronic hypoxia decreased.<sup>80</sup> Unfortunately, only 3 studies reported intracardiac lipid deposition of various lipids, which made meta-analysis impossible. Further research should aim for better understanding of the translational possibilities from experimental studies to human disease.

PGC1 $\alpha$  acts on transcription factors such as the PPARs and is an important transcription factor of mitochondrial content. Coactivation of PGC1 $\alpha$  with PPAR isoforms is known to induce activation of downstream genes regarding fatty acid handling including uptake and  $\beta$ -oxidation, especially fat transporter genes CD36 and CPT1B, and  $\beta$ -oxidation gene MCAD.<sup>81–84</sup> PPAR $\alpha$  is the most studied PPAR in the heart and this also applies for the pressure-loaded RV specifically.<sup>27,34,85</sup> Nevertheless, data of PPAR $\alpha$  expression in the pressure-loaded RV is still limited and mostly showing statistically insignificant results (Figure S4D). This is in contrast to PGC1 $\alpha$ , which is significantly negative affected in the pressure-loaded RV and seems to be related to mitochondrial content in models of RV pressure load. It must be mentioned that the different studies identified mitochondrial content using different methods, since standardized methods are lacking. Future studies should clarify whether decreased mitochondrial content indeed is predominately established in models of SuHx and to what extent this mechanism is relevant for human PH disease. Remarkably, both PGC1 $\alpha$  and PPAR $\alpha$  are not identified in studies with unbiased approach by performing microarray<sup>5,55,86–88</sup> or proteomics.<sup>87</sup> This could imply that changes of PGC1 $\alpha$  or PPAR $\alpha$  are not causal for altered processes caused by RV pressure load.

As shown in this review, metabolic modulation has been primarily focused on the reduction of glycolysis by activation of glucose oxidation. The most studied compound is dichloroacetate, which inhibits pyruvate dehydrogenase kinase and thereby indirectly stimulates activation of PDH. Interestingly, in the pressure-loaded RV, the different isoforms of pyruvate dehydrogenase kinase and PDH encompass varied results (Figures S2 and 5). However, studies specifically focusing on interfering in the activity of these enzymes in the pressure-loaded RV by dichloroacetate show positive effects on cell homeostasis, mitochondrial function, and cardiac function,<sup>15–17</sup> with no effect on these functions in controls.<sup>15</sup> In MCT and FHR, at respectively 6 weeks and >10 to 20 months of treatment, dichloroacetate leads to normalized levels of the upregulated PDK2 and PDK4, with restoration of PDH activity.<sup>16,17</sup> This was accompanied by normalization of FOXO1 levels, which were upregulated in disease in FHR animals and patients with PAH.<sup>16</sup> This is consistent with the concept of activation of the fetal gene program and insulin-independent mechanisms in the pressure-loaded RV, since sustained FOXO1 activation in neonatal cardiomyocytes is

known to diminish insulin signaling and impair glucose metabolism.<sup>89</sup>

## Limitations

This study has some limitations that should be discussed. To guarantee actual pressure load on the RV, meta-analysis includes both studies with proven increased pressure load by RV systolic pressure and mean pulmonary artery pressure, and by RVH. RVH was expressed as increased RV weight, Fulton index, or RV to body weight ratio. Although hypertrophy is a plausible effect of pressure load, the degree of hypertrophy within studies from the current literature search is independent of the actual degree of pressure load (data not shown). This might be explained by a predominant use of models of severe pressure load. This together with the fact that RVH based on weight is a widely supported confirmation of RV pressure overload resulted in RVH as an inclusion criterion in addition to increased pressure load.

In line with the statement of the Systematic Review Center for Laboratory animal Experimentation (SYRCLE),<sup>24</sup> the aim of this meta-analysis was to assess the general direction and magnitude of RV pressure load of the specific variable (rather than to obtain a precise point estimate explicitly) with additional exploration of the sources of heterogeneity by using meta-regression analyses. We used effect size defined as Hedges' *g*. Hedges' *g* is the criterion standard in small samples (<10 samples per group), which includes a correction factor for small sample size bias,<sup>90,91</sup> and therefore is considered as a criterion standard in meta-analysis of systematic reviews in animal data from experimental studies. However, we believe that the use of Hedges' *g* encompasses a specific point that should be addressed. Since the use of effect sizes implies standardized mean differences, calculations are based on a pooled SD, although unequal variances may be present. This may induce type I errors. However, the small and unequal sample sizes will likely cancel out this effect. An alternative statistic method would be statistics by using *Z* scores, but because we aimed to provide an overview of the results of the different studies, by the visualization by figures, this method was not preferred.

The interpretation of meta-analysis results were challenged by substantial degrees of heterogeneity, which was partly explored by performing (1) meta-regression analysis for duration and degree of pressure load, and (2) *t* tests or 1-way analysis of variance of the results of the different models. This resulted in 3 significant correlations with duration and various differences between models. Only 1 correlation was found with the degree of RV pressure load, which could be because of the fact that included studies encompass significant loading conditions. Systematically testing for the effect of used species was impossible because only 1 study

concerned animal species other than rat. This, however, contributed to large homogeneity at this particular point. Furthermore, we decided to use an almost similar approach for human as for animal studies in order to be able to apply the same methods regarding meta-analysis. Subsequently, a number of clinical studies were excluded from meta-analysis because of aspects regarding study design. Nevertheless, most of the excluded studies described FDG uptake and supported the presented results in the meta-analyses. Other human studies that were excluded from the meta-analyses described uptake of fatty acids, as has been described above.

## Considerations Regarding Future Research

Because of the use of differing designs of the included studies, the power of the meta-analysis is limited. In contrast to clinical trials, replication is still scarce in experimental research. The current study emphasizes the need for replication and the use of more standardization in models, methods, and outcome variables in studies that studied metabolic derangements in RV pressure load. This could be achieved in joint publications of different research groups. Available data describe to a certain extent the degree and duration of pressure load. In pursuing actual translation, absolute determination of pressure load will be necessary in both animals and humans, with the intention of differentiating between the actual component of pressure load and the cause of disease, including potential comorbidities. The cause of disease, or the character of the model, is important since models of PAH, such as hypoxia, SuHx, MCT, and FHR, may differ in their systemic effects and are known for differences in disease severity and cardiovascular interaction. These differences are driven by involvement of endothelial damage, level of inflammation, cytokine migration, and vasoconstriction. While isolated hypoxia with the absence of endothelial damage in the pulmonary vasculature induces mild PH only, FHR leads to more progressive PH, whereas SuHx and MCT will induce failure, with high rates of mortality in MCT. Exact mechanisms still need to be unraveled. The current meta-analysis directs to further exploration of the role of diseases that expose the RV to altered insulin sensitivity or oxygen tension in remodeling during RV pressure load. The current overview shows that determination of protein expression is limited compared with gene expression, and often shows divergent results. Also, measurements of substrate activities are relatively scarce. We suggest that future studies in the pressure-loaded RV should be more uniform and integral with respect to expression level (gene, protein, or activity level). The *variables of metabolism to be studied* should be uniform and those that are most optimal should be chosen based on research using unbiased approaches (ie, microarray, RNA sequences, proteomics, or

metabolomics). Given the abovementioned observations, the translational applicability between, and within, animal models and human diseases of PH should most critically and carefully be considered.

## Conclusions

This systematic review and meta-analysis of metabolic variables in the pressure-loaded RV showed a uniform increase in glucose uptake and glycolysis. Results regarding fatty acid uptake and changes in oxidative metabolism were divergent and model specific. To actually use metabolism as a therapeutic target in the RV exposed to increased pressure load in clinical practice, we need to learn more about model- and disease-specific mechanisms of fatty acid uptake and mitochondrial impairment.

## Disclosures

None.

## References

- Norози K, Wessel A, Alpers V, Arnhold JO, Geyer S, Zoega M, Buchhorn R. Incidence and risk distribution of heart failure in adolescents and adults with congenital heart disease after cardiac surgery. *Am J Cardiol.* 2006;97:1238–1243.
- Van Wolferen SA, Marcus JT, Boonstra A, Marques KMJ, Bronzwaer JGF, Spreeuwenberg MD, Postmus PE, Vonk-Noordegraaf A. Prognostic value of right ventricular mass, volume, and function in idiopathic pulmonary arterial hypertension. *Eur Heart J.* 2007;28:1250–1257.
- Ghio S, Gavazzi A, Campana C, Inserra C, Klersy C, Sebastiani R, Arbustini E, Recusani F, Tavazzi L. Independent and additive prognostic value of right ventricular systolic function and pulmonary artery pressure in patients with chronic heart failure. *J Am Coll Cardiol.* 2001;37:183–188.
- Meyer P, Filippatos GS, Ahmed MI, Iskandrian AE, Bittner V, Perry GJ, White M, Aban IB, Mujib M, Italia LJD, Ahmed A. Effects of right ventricular ejection fraction on outcomes in chronic systolic heart failure. *Circulation.* 2010;121:252–258.
- Borgdorff MAJ, Koop AMC, Bloks VW, Dickinson MG, Steendijk P, Sillje HHW, van Wiechen MPH, Berger RMF, Bartelds B. Clinical symptoms of right ventricular failure in experimental chronic pressure load are associated with progressive diastolic dysfunction. *J Mol Cell Cardiol.* 2015;79:244–253.
- Ryan JJ, Archer SL. The right ventricle in pulmonary arterial hypertension: disorders of metabolism, angiogenesis and adrenergic signaling in right ventricular failure. *Circ Res.* 2014;115:176–188.
- Borgdorff MAJ, Dickinson MG, Berger RMF, Bartelds B. Right ventricular failure due to chronic pressure load: What have we learned in animal models since the NIH working group statement? *Heart Fail Rev.* 2015;20:475–491.
- Samson N, Paulin R. Epigenetics, inflammation and metabolism in right heart failure associated with pulmonary hypertension. *Pulm Circ.* 2017;7:572–587.
- Koop AMC, Hagdorn QAJ, Bossers GPL, van Leusden T, Gerding A, van Weeghel M, Vaz FM, Koonen DPY, Sillje HHW, Berger RMF, Bartelds B. Right ventricular pressure overload alters cardiac lipid composition. *Int J Cardiol.* 2019;287:96–105.
- Bartelds B, Knoester H, Smid GB, Takens J, Visser GH, Penninga L, van der Leij FR, Beaufort-Krol GC, Zijlstra WG, Heymans HS, Kuipers JR. Perinatal changes in myocardial metabolism in lambs. *Circulation.* 2000;102:926–931.
- Bartelds B, Knoester H, Beaufort-Krol GC, Smid GB, Takens J, Zijlstra WG, Heymans HSA, Kuipers JRG. Myocardial lactate metabolism in fetal and newborn lambs. *Circulation.* 1999;99:1892–1897.
- Lopaschuk GD. Metabolic modulators in heart disease – Past Present and Future. *Can J Cardiol.* 2017;33:838–849.
- Neubauer S. The failing heart — an engine out of fuel. *N Engl J Med.* 2007;356:1140–1151.
- Sanz J, Sánchez-Quintana D, Bossone E, Bogaard HJ, Naeije R. Anatomy, function, and dysfunction of the right ventricle: JACC state-of-the-art review. *J Am Coll Cardiol.* 2019;73:1463–1482.
- Piao L, Fang Y-H, Cadete VJJ, Wietholt C, Urboniene D, Toth PT, Marsboom G, Zhang HJ, Haber I, Rehman J, Lopaschuk GD, Archer SL. The inhibition of pyruvate dehydrogenase kinase improves impaired cardiac function and electrical remodeling in two models of right ventricular hypertrophy: resuscitating the hibernating right ventricle. *J Mol Med.* 2010;88:47–60.
- Piao L, Sidhu VK, Fang Y-H, Ryan JJ, Parikh KS, Hong Z, Toth PT, Morrow E, Kutty S, Lopaschuk GD, Archer SL. FOXO1-mediated upregulation of pyruvate dehydrogenase kinase-4 (PDK4) decreases glucose oxidation and impairs right ventricular function in pulmonary hypertension: therapeutic benefits of dichloroacetate. *J Mol Med.* 2013;91:333–346.
- Sun X-Q, Zhang R, Zhang H-D, Yuan P, Wang X-J, Zhao Q-H, Wang L, Jiang R, Jan Bogaard H, Jing Z-C. Reversal of right ventricular remodeling by dichloroacetate is related to inhibition of mitochondria-dependent apoptosis. *Hypertens Res.* 2016;39:302–311.
- Piao L, Fang Y-H, Parikh K, Ryan JJ, Toth PT, Archer SL. Cardiac glutaminolysis: a maladaptive cancer metabolism pathway in the right ventricle in pulmonary hypertension. *J Mol Med.* 2013;91:1185–1197.
- Drozd K, Ahmadi A, Deng Y, Jiang B, Petryk J, Thorn S, Stewart D, Beanlands R, DeKemp RA, DaSilva JN, Mielniczuk LM. Effects of an endothelin receptor antagonist, Macitentan, on right ventricular substrate utilization and function in a Sugen 5416/hypoxia rat model of severe pulmonary arterial hypertension. *J Nucl Cardiol.* 2016;24:1–11.
- Liu A, Philip J, Vinnakota KC, Van den Bergh F, Tabima DM, Hacker T, Beard DA, Chesler NC. Estrogen maintains mitochondrial content and function in the right ventricle of rats with pulmonary hypertension. *Physiol Rep.* 2017;5:1–12.
- Fang Y-H, Piao L, Hong Z, Toth PT, Marsboom G, Bache-Wiig P, Rehman J, Archer SL. Therapeutic inhibition of fatty acid oxidation in right ventricular hypertrophy: exploiting Randle's cycle. *J Mol Med.* 2012;90:31–43.
- Khan SS, Cuttica MJ, Beussink-Nelson L, Kozyleva A, Sanchez C, Mkrdichian H, Selvaraj S, Dematte JE, Lee DC, Shah SJ. Effects of ranolazine on exercise capacity, right ventricular indices, and hemodynamic characteristics in pulmonary arterial hypertension: a pilot study. *Pulm Circ.* 2015;5:547–556.
- Michelakis ED, Gurtu V, Webster L, Barnes G, Watson G, Howard L, Cupitt J, Paterson I, Thompson RB, Chow K, Regan DPO, Zhao L, Wharton J, Kiely DG, Kinnaird A, Boukouris AE, White C, Nagendran J, Freed DH, Wort SJ, Gibbs JSR, Wilkins MR. Inhibition of pyruvate dehydrogenase kinase improves pulmonary arterial hypertension in genetically susceptible patients. *Sci Transl Med.* 2017;4583:1–13.
- de Vries RBM, Hooijmans CR, Langendam MW, van Luijk J, Leenaars M. A protocol format for the preparation, registration and publication of systematic reviews of animal intervention studies. *Evidenc Based Preclin Med.* 2015;1:e00007.
- De Vries RBM, Wever KE, Avey MT, Stephens ML, Sena ES, Leenaars M. The usefulness of systematic reviews of animal experiments for the design of preclinical and clinical studies. *ILAR J.* 2014;55:427–437.
- Galiè N, Hoepfer MM, Humbert M, Torbicki A, Vachiery JL, Barbera JA, Beghetti M, Corris P, Gaine S, Gibbs JS, Gomez-Sanchez MA, Jordeau G, Klepetko W, Opitz C, Peacock A, Rubin L, Zellweger M, Simonneau G. Guidelines for the diagnosis and treatment of pulmonary hypertension. *Eur Respir J.* 2009;34:1219–1263.
- Gomez-Arroyo J, Mizuno S, Szczepanek K, Van Tassel B, Natarajan R, Dos Remedios CG, Drake JI, Farkas L, Kraskauskas D, Wijesinghe DS, Chalfant CE, Bigbee J, Abbate A, Lesnefsky EJ, Bogaard HJ, Voelkel NF. Metabolic gene remodeling and mitochondrial dysfunction in failing right ventricular hypertrophy secondary to pulmonary arterial hypertension. *Circ Heart Fail.* 2013;6:136–144.
- Balestra GM, Mik EG, Eerbeek O, Specht PAC, van der Laarse WJ, Zuurbier CJ. Increased in vivo mitochondrial oxygenation with right ventricular failure induced by pulmonary arterial hypertension: mitochondrial inhibition as driver of cardiac failure? *Respir Res.* 2015;16:6.
- Rumsey WL, Abbott B, Bertelsen D, Mallamaci M, Hagan K, Nelson D, Erecinska M. Adaptation to hypoxia alters energy metabolism in rat heart. *Am J Physiol.* 1999;276:H71–H80.
- Zhang W-H, Qiu M-H, Wang X-J, Sun K, Zheng Y, Jing Z-C. Up-regulation of hexokinase1 in the right ventricle of monocrotaline induced pulmonary hypertension. *Respir Res.* 2014;15:119.
- Graham BB, Kumar R, Mickael C, Sanders L, Gebreab L, Huber KM, Perez M, Smith-Jones P, Serkova NJ, Tuder RM. Severe pulmonary hypertension is associated with altered right ventricle metabolic substrate uptake. *Am J Physiol.* 2015;309:L435–L440.

32. Sutendra G, Dromparis P, Paulin R, Zervopoulos S, Haromy A, Nagendran J, Michelakakis ED. A metabolic remodeling in right ventricular hypertrophy is associated with decreased angiogenesis and a transition from a compensated to a decompensated state in pulmonary hypertension. *J Mol Med*. 2013;91:1315–1327.
33. Wang L, Li W, Yang Y, Wu W, Cai Q, Ma X, Xiong C, He J, Fang W. Quantitative assessment of right ventricular glucose metabolism in idiopathic pulmonary arterial hypertension patients: a longitudinal study. *Eur Heart J Cardiovasc Imaging*. 2016;17:1161–1168.
34. Adroge JV, Sharma S, Ngumbela K, Essop MF, Taegtmeier H. Acclimatization to chronic hypobaric hypoxia is associated with a differential transcriptional profile between the right and left ventricle. *Mol Cell Biochem*. 2005;278:71–78.
35. Sharma S, Taegtmeier H, Adroge J, Razeghi P, Sen S, Ngumbela K, Essop MF. Dynamic changes of gene expression in hypoxia-induced right ventricular hypertrophy. *Am J Physiol*. 2004;286:H1185–H1192.
36. Sivitz WI, Lund DD, Yorek B, Grover-McKay M, Schmid PG. Pretranslational regulation of two cardiac glucose transporters in rats exposed to hypobaric hypoxia. *Am J Physiol*. 1992;263:E562–E569.
37. van der Bruggen CE, Happé CM, Dorfmueller P, Trip P, Spruijt OA, Rol N, Hoevenaars FP, Houweling AC, Girerd B, Marcus JT, Mercier O, Humbert M, Handoko ML, van der Velden J, Vonk Noordegraaf A, Bogaard HJ, Goumans M-J, de Man FS. Bone morphogenetic protein receptor type 2 mutation in pulmonary arterial hypertension: a view on the right ventricle. *Circulation*. 2016;133:1747–1760.
38. Bruns DR, Dale Brown R, Stenmark KR, Buttrick PM, Walker LA. Mitochondrial integrity in a neonatal bovine model of right ventricular dysfunction. *Am J Physiol*. 2015;308:L158–L167.
39. Paulin R, Sutendra G, Gurtu V, Dromparis P, Haromy A, Provencher S, Bonnet S, Michelakakis ED. A miR-208-Mef2 axis drives the decompensation of right ventricular function in pulmonary hypertension. *Circ Res*. 2015;116:56–69.
40. Broderick TL, King TM. Upregulation of GLUT-4 in right ventricle of rats with monocrotaline-induced pulmonary hypertension. *Med Sci Monit*. 2008;14:BR261–BR264.
41. Talati MH, Brittain EL, Fessel JP, Penner N, Atkinson J, Funke M, Grueter C, Jerome WG, Freeman M, Newman JH, West J, Hemnes AR. Mechanisms of lipid accumulation in the bone morphogenetic protein receptor type 2 mutant right ventricle. *Am J Respir Crit Care Med*. 2016;194:719–728.
42. Nouette-Gaulain K, Malgat M, Rocher C, Savineau J-P, Marthan R, Mazat J-P, Sztark F. Time course of differential mitochondrial energy metabolism adaptation to chronic hypoxia in right and left ventricles. *Cardiovasc Res*. 2005;66:132–140.
43. Enache I, Charles A-L, Bouitbir J, Favret F, Zoll J, Metzger D, Oswald-Mammosser M, Geny B, Charloux A. Skeletal muscle mitochondrial dysfunction precedes right ventricular impairment in experimental pulmonary hypertension. *Mol Cell Biochem*. 2013;373:161–170.
44. Lauva IK, Brody E, Tiger E, Kent RL, Copper G IV, Marino TA. Control of myocardial tissue components and cardiocyte organelles in pressure-overload hypertrophy of the cat right ventricle. *Am J Anat*. 1986;177:71–80.
45. Olivetti G, Ricci R, Lagrasta C, Maniga E, Sonnenblick EH, Anversa P. Cellular basis of wall remodeling in long-term pressure overload-induced right ventricular hypertrophy in rats. *Circ Res*. 1988;63:648–657.
46. Sack MN, Disch DL, Rockman HA, Kelly DP. A role for Sp and nuclear receptor transcription factors in a cardiac hypertrophic growth program. *Proc Natl Acad Sci USA*. 1997;94:6438–6443.
47. Sheikh AM, Barrett C, Villamizar N, Alzate O, Valente AM, Herlong JR, Craig D, Lodge A, Lawson J, Milano C, Jagers J. Right ventricular hypertrophy with early dysfunction: a proteomics study in a neonatal model. *J Thorac Cardiovasc Surg*. 2009;137:1146–1153.
48. Mccommis KS, Douglas DL, Krenz M, Baines CP. Cardiac-specific hexokinase 2 overexpression attenuates hypertrophy by increasing pentose phosphate pathway flux. *J Am Heart Assoc*. 2013;2:e000355. DOI: 10.1161/JAHA.113.000355.
49. Wu R, Wyatt E, Chawla K, Tran M, Ghanefar M, Laakso M, Epting CL, Ardehali H. Hexokinase II knockdown results in exaggerated cardiac hypertrophy via increased ROS production. *EMBO Mol Med*. 2012;4:633–646.
50. Calmettes G, John SA, Weiss JN, Ribalet B. Hexokinase—mitochondrial interactions regulate glucose metabolism differentially in adult and neonatal cardiac myocytes. *J Gen Physiol*. 2013;142:425–436.
51. Gottlob K, Majewski N, Kennedy S, Kandel E, Robey RB, Hay N. Inhibition of early apoptotic events by Akt/PKB is dependent on the first committed step of glycolysis and mitochondrial hexokinase. *Genes Dev*. 2001;15:1406–1418.
52. Fritz HL, Smoak IW, Branch S. Hexokinase I expression and activity in embryonic mouse heart during early and late organogenesis. *Histochem Cell Biol*. 1999;112:359–365.
53. St John JC, Ramalho-Santos J, Gray HL, Petrosko P, Rawe VY, Navara CS, Simerly CR, Schatten GP. The expression of mitochondrial DNA transcription factors during early cardiomyocyte *in vitro* differentiation from human embryonic stem cells. *Cloning Stem Cells*. 2005;7:141–153.
54. Reddy S, Zhao M, Hu D-Q, Fajardo G, Katznelson E, Punn R, Spin JM, Chan FP, Bernstein D. Physiologic and molecular characterization of a murine model of right ventricular volume overload. *Am J Physiol Heart Circ Physiol*. 2013;304:H1314–H1327.
55. Reddy S, Zhao M, Hu D-Q, Fajardo G, Hu S, Ghosh Z, Rajagopalan V, Wu JC, Bernstein D. Dynamic microRNA expression during the transition from right ventricular hypertrophy to failure. *Physiol Genomics*. 2012;44:562–575.
56. Drake JJ, Bogaard HJ, Mizuno S, Clifton B, Xie B, Gao Y, Dumur CI, Fawcett P, Voelkel NF, Natarajan R. Molecular signature of a right heart failure program in chronic severe pulmonary hypertension. *Am J Respir Cell Mol Biol*. 2011;45:1239–1247.
57. Postic C, Leturque A, Printz RL, Maulard P, Loizeau M, Granner DK, Girard J. Development and regulation of glucose transporter and hexokinase expression in rat. *Am J Physiol*. 1994;266:E548–E559.
58. Frille A, Steinhoff KG, Hesse S, Grachtrup S, Wald A, Wirtz H, Sabri O, Seyfarth H-J. Thoracic [18F]fluorodeoxyglucose uptake measured by positron emission tomography/computed tomography in pulmonary hypertension. *Med (Baltimore)*. 2016;95:e3976.
59. Ohira H, deKemp R, Pena E, Davies RA, Stewart DJ, Chandy G, Contreras-Dominguez V, Dennie C, Mc Ardle B, Mc Klein R, Renaud JM, DaSilva JN, Pugliese C, Dunne R, Beanlands R, Mielniczuk LM. Shifts in myocardial fatty acid and glucose metabolism in pulmonary arterial hypertension: a potential mechanism for a maladaptive right ventricular response. *Eur Heart J Cardiovasc Imaging*. 2016;17:1424–1431.
60. Sakao S, Daimon M, Voelkel NF, Miyachi H, Jujo T, Sugiura T, Ishida K, Tanabe N, Kobayashi Y, Tatsumi K. Right ventricular sugars and fats in chronic thromboembolic pulmonary hypertension. *Int J Cardiol*. 2016;219:143–149.
61. Bokhari S, Raina A, Rosenweig EB, Schulze PC, Bokhari J, Einstein AJ, Barst RJ, Johnson LL. PET imaging may provide a novel biomarker and understanding of right ventricular dysfunction in patients with idiopathic pulmonary arterial hypertension. *Circ Cardiovasc Imaging*. 2011;4:641–647.
62. Saygin D, Highland KB, Farha S, Park M, Sharp J, Roach EC, Tang WHW, Thomas JD, Erzurum SC, Neumann DR, DiFilippo FP. Metabolic and functional evaluation of the heart and lungs in pulmonary hypertension by gated 2-[18F]-Fluoro-2-deoxy-D-glucose positron emission tomography. *Pulm Circ*. 2017;7:428–438.
63. Nakaya T, Ohira H, Tsujino I. Right heart morphology, function and metabolism in pulmonary hypertension. *Respir Circ*. 2016;64:543–547.
64. Oikawa M, Kagaya Y, Otani H, Sakuma M, Demachi J, Suzuki J, Takahashi T, Nawata J, Ido T, Watanabe J, Shirato K. Increased [18F]fluorodeoxyglucose accumulation in right ventricular free wall in patients with pulmonary hypertension and the effect of epoprostenol. *J Am Coll Cardiol*. 2005;45:1849–1855.
65. Lundgrin EL, Park MM, Sharp J, Tang WHW, Thomas JD, Asosingh K, Comhair SA, DiFilippo FP, Neumann DR, Davis L, Graham BB, Tuder RM, Dostanic I, Erzurum SC. Fasting 2-deoxy-2-[18F]fluoro-D-glucose positron emission tomography to detect metabolic changes in pulmonary arterial hypertension hearts over 1 year. *Ann Am Thorac Soc*. 2013;10:1–9.
66. Li W, Wang L, Xiong C-M, Yang T, Zhang Y, Gu Q, Yang Y, Ni X-H, Liu Z-H, Fang W, He J-G. The prognostic value of 18F-FDG uptake ratio between the right and left ventricle in idiopathic pulmonary arterial hypertension. *Clin Nucl Med*. 2015;40:859–863.
67. Tatebe S, Fukumoto Y, Oikawa-Wakayama M, Sugimura K, Satoh K, Miura Y, Aoki T, Nochioka K, Miura M, Yamamoto S, Tashiro M, Kagaya Y, Shimokawa H. Enhanced [18F]fluorodeoxyglucose accumulation in the right ventricular free wall predicts long-term prognosis of patients with pulmonary hypertension: a preliminary observational study. *Eur Heart J Cardiovasc Imaging*. 2014;15:666–672.
68. Faber MJ, Dalinghaus M, Lankhuizen IM, Bezstarosti K, Verhoeven AJM, Duncker DJ, Helbing WA, Lamers MJM. Time dependent changes in cytoplasmic proteins of the right ventricle during prolonged pressure overload. *J Mol Cell Cardiol*. 2007;43:197–209.
69. Baandrup JD, Markvardsen LH, Peters CD, Schou UK, Jensen JL, Magnusson NE, Ørntoft TF, Kruhoffer M, Simonsen U. Pressure load: the main factor for altered gene expression in right ventricular hypertrophy in chronic hypoxic rats. *PLoS One*. 2011;6:e15859.
70. Faber MJ, Dalinghaus M, Lankhuizen IM, Bezstarosti K, Dekkers DHW, Duncker DJ, Helbing WA, Lamers MJM. Proteomic changes in the pressure overloaded right ventricle after 6 weeks in young rats: Correlations with the degree of hypertrophy. *Proteomics*. 2005;5:2519–2530.
71. Wong YY, Rajmakers P, Van Campen J, Van Der Laarse WJ, Knaepen P, Lubberink M, Rüter G, Noordegraaf AV, Lammertsma AA. 11C-acetate

- clearance as an index of oxygen consumption of the right myocardium in idiopathic pulmonary arterial hypertension: a validation study using 15O-labeled tracers and PET. *J Nucl Med*. 2013;54:1258–1262.
72. Yoshinaga K, Ohira H, Tsujino I, Oyama-Manabe N, Mielniczuk L, Beanlands RSB, Katoh C, Kasai K, Manabe O, Sato T, Fujii S, Ito YM, Tomiyama Y, Nishimura M, Tamaki N. Attenuated right ventricular energetics evaluated using 11C-acetate PET in patients with pulmonary hypertension. *Eur J Nucl Med Mol Imaging*. 2014;41:1240–1250.
  73. Matsushita T, Ikeda S, Miyahara Y, Yakabe K, Yamaguchi K, Furukawa K, Iwasaki T, Shikuwa M, Fukui J, Kohno S. Use of [123I]-BMIPP myocardial scintigraphy for the clinical evaluation of a fatty-acid metabolism disorder of the right ventricle in chronic respiratory and pulmonary vascular disease. *J Int Med Res*. 2000;28:111–123.
  74. Sakao S, Miyauchi H, Voelkel NF, Sugiura T, Tanabe N, Kobayashi Y, Tatsumi K. Increased right ventricular fatty acid accumulation in chronic thromboembolic pulmonary hypertension. *Ann Am Thorac Soc*. 2015;12:1465–1472.
  75. Nagaya N, Goto Y, Satoh T, Uematsu M, Hamada S, Kuribayashi S, Okano Y, Kyotani S, Shimotsu Y, Fukuchi K, Nakanishi N, Takamiya M, Ishida Y. Impaired regional fatty acid uptake and systolic dysfunction in hypertrophied right ventricle. *J Nucl Med*. 1998;39:1676–1680.
  76. Drake JI, Gomez-Arroyo J, Dumur CI, Kraskauskas D, Natarajan R, Bogaard HJ, Fawcett P, Voelkel NF. Chronic carvedilol treatment partially reverses the right ventricular failure transcriptional profile in experimental pulmonary hypertension. *Physiol Genomics*. 2013;45:449–461.
  77. Lewandowski ED, Fischer SK, Fasano M, Banke NH, Walker LA, Huqi A, Wang X, Lopaschuk GD, O'Donnell JM. Acute liver carnitine palmitoyltransferase I overexpression recapitulates reduced palmitate oxidation of cardiac hypertrophy. *Circ Res*. 2013;112:57–65.
  78. Talati M, Hemnes A. Fatty acid metabolism in pulmonary arterial hypertension: role in right ventricular dysfunction and hypertrophy. *Pulm Circ*. 2015;5:269–278.
  79. Brittain EL, Talati M, Fessel JP, Zhu H, Penner N, Calcutt MW, West JD, Funke M, Lewis GD, Gerszten RE, Hamid R, Pugh ME, Austin ED, Newman JH, Hemnes AR. Fatty acid metabolic defects and right ventricular lipotoxicity in human pulmonary arterial hypertension. *Circulation*. 2016;133:1936–1944.
  80. Bitar FF, Bitar H, El Sabban M, Nasser M, Yunis KA, Tawil A, Dbaibo GS. Modulation of ceramide content and lack of apoptosis in the chronically hypoxic neonatal rat heart. *Pediatr Res*. 2002;51:144–149.
  81. Huss JM, Gigue V, Kelly DP. Estrogen-related receptor alpha directs peroxisome proliferator-activated receptor alpha signaling in the transcriptional control of energy metabolism in cardiac and skeletal muscle. *Society*. 2004;24:9079–9091.
  82. Burkart EM, Welch MJ, Kelly DP, Burkart EM, Sambandam N, Han X. Nuclear receptors PPAR b/d and PPAR a direct distinct metabolic regulatory programs in the mouse heart Find the latest version: nuclear receptors PPAR  $\beta/\delta$  and PPAR  $\alpha$  direct distinct metabolic regulatory programs in the mouse heart. *J Clin Invest*. 2007;117:3930–3939.
  83. Yang J, Sambandam N, Han X, Gross RW, Courtois M, Kovacs A, Febbraio M, Finck BN, Kelly DP. CD36 deficiency rescues lipotoxic cardiomyopathy. *Circ Res*. 2007;100:1208–1217.
  84. Duncan JG, Bharadwaj KG, Fong JL, Mitra R, Sambandam N, Courtois MR, Lavine KJ, Goldberg IJ, Kelly DP. Rescue of cardiomyopathy in peroxisome proliferator-activated receptor-alpha transgenic mice by deletion of lipoprotein lipase identifies sources of cardiac lipids and peroxisome proliferator-activated receptor-a activators. *Circulation*. 2010;121:426–435.
  85. Sharma S, Adrogue JV, Golfman L, Uray I, Lemm J, Youker K, Noon GP, Frazier OH, Taegtmeyer H. Intramyocardial lipid accumulation in the failing human heart resembles the lipotoxic rat heart. *FASEB J*. 2004;18:1692–1700.
  86. Urashima T, Zhao M, Wagner R, Fajardo G, Farahani S, Quertermous T, Bernstein D, Quertermous T, Molecular BD. Molecular and physiological characterization of RV remodeling in a murine model of pulmonary stenosis. *Am J Physiol Heart Circ Physiol*. 2008;295:H1351–H1368.
  87. Friehs I, Cowan DB, Choi Y-H, Black KM, Barnett R, Bhasin MK, Daly C, Dillon SJ, Libermann TA, McGowan FX, del Nido PJ, Levitsky S, McCully JD. Pressure-overload hypertrophy of the developing heart reveals activation of divergent gene and protein pathways in the left and right ventricular myocardium. *Am J Physiol Heart Circ Physiol*. 2013;304:H697–H708.
  88. Kreymborg Kc, Uchida S, Gellert P, Schneider A, Boettger T, Voswinckel R, Wietelmann A, Szibor M, Weissmann N, Ghofrani AH, Schermuly R, Schranz D, Seeger W, Braun T. Identification of right heart-enriched genes in a murine model of chronic outflow tract obstruction. *J Mol Cell Cardiol*. 2010;49:598–605.
  89. Ni YG, Wang N, Cao DJ, Sachan N, Morris DJ, Gerard RD, Kuro-o M, Rothermel BA, Hill JA. FoxO transcription factors activate Akt and attenuate insulin signaling in heart by inhibiting protein phosphatases. *Proc Natl Acad Sci*. 2007;104:20517–20522.
  90. Hedges L, Olkin I. *Statistical methods for meta-analysis*. Orlando: Academic Press; 1985.
  91. Vesterinen HM, Sena ES, Egan KJ, Hirst TC, Churolov L, Currie GL, Antonic A, Howells DW, Macleod MR. Meta-analysis of data from animal studies: a practical guide. *J Neurosci Methods*. 2014;221:92–102.



# SUPPLEMENTAL MATERIAL

## Data S1.

### Supplemental Methods

#### Search strategy

##### 1. Component 'right ventricle'

"right ventricle"[tiab] OR "right ventricles"[tiab] OR "right ventricular"[tiab] OR "ventriculus dexter"[tiab] OR "right heart"[tiab] OR "RV"[tiab]

##### 2. Component 'pressure load'

"pressure load"[tiab] OR "pressure loading"[tiab] OR "pressure loaded"[tiab] OR "pressure loads"[tiab] OR "pressure overload"[tiab] OR "pressure overloading"[tiab] OR "pressure overloaded"[tiab] OR "pressure overloads"[tiab] OR "increased afterload"[tiab] OR "increased afterloading"[tiab] OR "afterloaded"[tiab] OR "increased afterloads"[tiab] OR "pulmonary artery banding"[tiab] OR "pulmonary hypertension"[tiab] OR "pulmonary arterial hypertension"[tiab] OR "pulmonary valve stenosis"[tiab] OR "pulmonary valve calcification"[tiab] OR "calcification pulmonary valve"[tiab] OR "pulmonary valve diseases"[tiab] OR "pulmonary valve disease"[tiab] OR "pulmonary stenosis"[tiab] OR "stenosis pulmonary valve"[tiab] OR "pulmonary outflow tract obstruction"[tiab] OR "obstruction pulmonary outflow tract"[tiab] OR "pulmonary artery obstruction"[tiab] OR "pulmonary artery stenosis"[tiab]

##### 3. Component 'metabolism'

"metabolism"[tiab] OR "metabolic"[tiab] OR "energy metabolism"[tiab] OR "basal metabolism"[tiab] OR "carbohydrate metabolism"[tiab] OR "metabolic network"[tiab] OR "metabolic pathways"[tiab] OR "metabolic networks and pathways"[tiab] OR "biosynthetic pathways"[tiab] OR "metabolic activation"[tiab] OR "metabolic inactivation"[tiab] OR "secondary metabolism"[tiab] OR "metabolic remodeling"[tiab] OR "metabolic remodelling"[tiab] OR "metabolic"[tiab] OR "metabolic reprogramming"[tiab] OR "metabolite"[tiab] OR "metabolomic"[tiab] OR "metabolomics"[tiab] OR "metabolite profile"[tiab] OR "metabolites profiles"[tiab] OR "metabolite derangements"[tiab] OR "metabolomic signatures"[tiab] OR "substrate flux"[tiab] OR "mitochondria"[tiab] OR "mitochondrial"[tiab] OR "mitochondrion"[tiab] OR "mitochondrial energy transduction"[tiab] OR "glucose metabolism"[tiab] OR "glucose oxidation"[tiab] OR "gluconeogenesis"[tiab] OR "glycogenolysis"[tiab] OR "glycolysis"[tiab] OR "glycosylation"[tiab] OR "pyruvate"[tiab] OR "glucose"[tiab] OR "pentose phosphate pathway"[tiab] OR "fatty acid"[tiab] OR "fatty acids"[tiab] OR "long chain fatty acids"[tiab] OR "lipid metabolism"[tiab] OR "lipolysis"[tiab] OR "lipoylation"[tiab] OR "fatty acid oxidation"[tiab] OR "lipotoxicity"[tiab] OR "triglyceride"[tiab] OR "ceramide"[tiab] OR "lipid deposition"[tiab] OR "beta-oxidation"[tiab] OR "beta oxidation"[tiab] OR "fatty acid transport"[tiab] OR " $\beta$ -oxidation"[tiab] OR "branched chain amino acids"[tiab] OR "branched chain amino acid"[tiab] OR "amino acid"[tiab] OR "amino acids"[tiab] OR "BCAA"[tiab] OR "branched chain aminotransferase"[tiab] OR "branched-chain aminotransferase"[tiab] OR "BCAT"[tiab] OR "brached chain keto acids"[tiab] OR "brached-chain keto acids"[tiab] OR "BCKA"[tiab] OR "BCKA dehydrogenase complex"[tiab] OR "BCKD"[tiab] OR "ketone"[tiab] OR "ketones"[tiab] OR "ketogenesis"[tiab] OR "ketosis"[tiab] OR "ketone body"[tiab] OR "citric acid cycle"[tiab] OR "tricarboxylic acid cycle"[tiab] OR "TCA cycle"[tiab] OR "Krebs cycle"[tiab] OR "ATP"[tiab] OR "ADP"[tiab] OR "adenosine diphosphate"[tiab] OR "adenosine triphosphate"[tiab] OR "respiratory transport"[tiab] OR "oxidation-reduction"[tiab] OR "oxidative phosphorylation"[tiab] OR "phosphorylation"[tiab] OR "electron transport"[tiab] OR "electron transport chain"[tiab] OR "metabolic targets"[tiab] OR "metabolic therapy"[tiab] OR "fatty acid oxidation inhibitor"[tiab] OR "glucose oxidation inhibitor"[tiab] OR "fatty acid uptake inhibitor"[tiab] OR "metabolic inhibitor"[tiab] OR "metabolic activator"[tiab] OR "inhibition of metabolic pathways"[tiab] OR "inhibition of

metabolic pathway"[tiab] OR "metabolic inducers"[tiab] OR "metabolic inducer"[tiab] OR "metabolic inducement"[tiab] OR "metabolic activation"[tiab] OR "metabolic regulation"[tiab] OR "regulation of metabolism"[tiab] OR "regulation of fatty acid"[tiab] OR "regulation of fatty acids"[tiab] OR "stimulation of fatty acid metabolism"[tiab] OR "inhibition of fatty acid metabolism"[tiab] OR "regulation of glucose oxidation"[tiab] OR "regulation of glycolysis"[tiab] OR "stimulation of glucose oxidation"[tiab] OR "inhibition of glycolysis"[tiab] OR "inhibition of glucose oxidation"[tiab] OR "amino acid administration"[tiab] OR "amino acids administration"[tiab] OR "metabolic defect"[tiab] OR "catabolic defect"[tiab] OR "cell respiration"[tiab] OR "cell hypoxia"[tiab] OR "respiratory burst"[tiab] OR "anaerobiosis"[tiab] OR "oxidative stress"[tiab]

**Table S1. List of studies studying metabolic parameters in the pressure loaded right ventricle included for full text review.**

Author	Year	Title	PMID	Embase Accession ID	Animal	Human	Specie	Model	Disease	Inclusion meta- analysis
Cooper, et al. <sup>1</sup>	1974	Normal myocardial function and energetics after reversing pressure overload hypertrophy	4274811	1975096311	x		cat	PAB		
Cooper, et al. <sup>2</sup>	1981	Chronic progressive pressure overload of the cat right ventricle.	6450649		x		cat	PAB		
Reibel, et al. <sup>3</sup>	1983	Altered coenzyme A and carnitine metabolism in pressure-overload hypertrophied hearts.	6222659		x		cat			
Lauva, et al. <sup>4</sup>	1986	Control of myocardial tissue components and cardiocyte organelles in pressure-overload hypertrophy of the cat right ventricle.	2877565		x		cat	PAB		x
Schneider, et al. <sup>5</sup>	1987	Development and regression of right heart ventricular hypertrophy: biochemical and morphological aspects.	2963447		x					
Olivetti, et al. <sup>6</sup>	1988	Cellular basis of wall remodeling in long-term pressure overload-induced right ventricular hypertrophy in rats.	2970334		x		rat	PAB		x
Hung, et al. <sup>7</sup>	1988	Morphometry of right ventricular papillary muscle in rat during development and regression of hypoxia-induced hypertension.	3381706		x					
Saito, et al. <sup>8</sup>	1991	Oxygen metabolism of the hypertrophic right ventricle in open chest dogs.	1839241		x		dog	PAB		
Morioka, et al. <sup>9</sup>	1992	Changes in contractile and non-contractile proteins, intracellular Ca <sup>2+</sup> and ultrastructures during the development of right ventricular hypertrophy and failure	1534855		x		rat	MCT60		

		in rats.						
Sivitz, et al. <sup>10</sup>	1992	Pretranslational regulation of two cardiac glucose transporters in rats exposed to hypobaric hypoxia.	1415537	x		rat	hypoxia	x
Baudet, et al. <sup>11</sup>	1994	Biochemical, mechanical and energetic characterization of right ventricular hypertrophy in the ferret heart.	7731052	x		ferret	PAC	
Ishikawa, et al. <sup>12</sup>	1995	Enalapril improves heart failure induced by monocrotaline without reducing pulmonary hypertension in rats: roles of preserved myocardial creatine kinase and lactate dehydrogenase isoenzymes.	7721499	x		rat	MCT50	
Do, et al. <sup>13</sup>	1995	Intracellular pH during hypoxia in normal and hypertrophied right ventricle of ferret heart.	7602610	x		ferret	PAB	
Sack, et al. <sup>14</sup>	1997	A role for Sp and nuclear receptor transcription factors in a cardiac hypertrophic growth program.	9177236	x		mouse	PAB	x
Nagaya, et al. <sup>15</sup>	1998	Impaired regional fatty acid uptake and systolic dysfunction in hypertrophied right ventricle.	9776267		x			PH (mPAP > 20)
Rumsey, et al. <sup>16</sup>	1999	Adaptation to hypoxia alters energy metabolism in rat heart.	9887019	x		rat	hypoxia	x
O'Brien, et al. <sup>17</sup>	1999	F1-ATP synthase beta-subunit and cytochrome c transcriptional regulation in right ventricular hemodynamic overload and hypertrophically stimulated cardiocytes.	10072725	x		feline (cat)	PAB	
Matsushita, et al. <sup>18</sup>	2000	Use of [123I]-BMIPP myocardial scintigraphy for the clinical evaluation of a fatty-acid metabolism disorder of the right ventricle in chronic respiratory and pulmonary vascular disease.	10983861		x			RVPO
Bitar, et al. <sup>19</sup>	2002	Modulation of ceramide content and lack of apoptosis in the chronically hypoxic neonatal rat heart.	11809907	x		rat	hypoxia	

Ecarnot-Laubreit, et al. <sup>20</sup>	2003	The activation pattern of the antioxidant enzymes in the right ventricle of rat in response to pressure overload is of heart failure type.	14503927	x	rat	MCT60	
Farahmand, et al. <sup>21</sup>	2004	Antioxidant and oxidative stress changes in experimental cor pulmonale.	15228082	x	rat	MCT60	
Cisar, et al. <sup>22</sup>	2004	Differential expression of mitochondrial electron transport chain proteins in cardiac tissues of broilers from pulmonary hypertension syndrome-resistant and -susceptible lines.	15339019	x	broiler	hypoxia	
Sharma, et al. <sup>23</sup>	2004	Dynamic changes of gene expression in hypoxia-induced right ventricular hypertrophy.	14630626	x	rat	hypoxia	x
Nouette-Gaulain, et al. <sup>24</sup>	2004	Time course of differential mitochondrial energy metabolism adaptation to chronic hypoxia in right and left ventricles.	15769456	x	rat	hypoxia	x
Adroque, et al. <sup>25</sup>	2005	Acclimatization to chronic hypobaric hypoxia is associated with a differential transcriptional profile between the right and left ventricle.	16180091	x	rat	hypoxia	x
van Beek-Harmsen and van der Laarse <sup>26</sup>	2005	Immunohistochemical determination of cytosolic cytochrome C concentration in cardiomyocytes.	15995138	x	rat	MCT40	
Schott, et al. <sup>27</sup>	2005	Pressure overload and neurohumoral activation differentially affect the myocardial proteome.	15732135	x	rat	MCT50	
Faber, et al. <sup>28</sup>	2005	Proteomic changes in the pressure overloaded right ventricle after 6 weeks in young rats: correlations with the degree of hypertrophy.	15912512	x	rat	PAB	
Kluge, et al. <sup>29</sup>	2005	Different mechanisms for changes in glucose uptake of the right and left ventricular myocardium in pulmonary hypertension.	15632029				x PH

Oikawa, et al. <sup>30</sup>	2005	Increased [18F]fluorodeoxyglucose accumulation in right ventricular free wall in patients with pulmonary hypertension and the effect of epoprostenol.	15936618		x				PH
Redout, et al. <sup>31</sup>	2007	Right-ventricular failure is associated with increased mitochondrial complex II activity and production of reactive oxygen species.	17582388		x	rat	MCT80		
Faber, et al. <sup>32</sup>	2007	Time dependent changes in cytoplasmic proteins of the right ventricle during prolonged pressure overload.	17603072		x	rat	PAB		
Basu, et al. <sup>33</sup>	2007	Etiopathologies associated with intercostal muscle hypermetabolism and prominent right ventricle visualization on 2-deoxy-2[F-18]fluoro-D-glucose-positron emission tomography: significance of an incidental finding and in the setting of a known pulmonary disease.	17610018		x				Varied diseases
Nagendran, et al. <sup>34</sup>	2008	A dynamic and chamber-specific mitochondrial remodeling in right ventricular hypertrophy can be therapeutically targeted.	18603070		x	rat	MCT		
Broderick and King. <sup>35</sup>	2008	Upregulation of GLUT-4 in right ventricle of rats with monocrotaline-induced pulmonary hypertension.	19043358		x	rat	MCT60		x
Mouchaers, et al. <sup>36</sup>	2009	Endothelin receptor blockade combined with phosphodiesterase-5 inhibition increases right ventricular mitochondrial capacity in pulmonary arterial hypertension.	19395550		x	rat	MCT40		
Sheikh, et al. <sup>37</sup>	2009	Right ventricular hypertrophy with early dysfunction: A proteomics study in a neonatal model.	19379982		x	piglet	PAB		x
Redout, et al. <sup>38</sup>	2010	Antioxidant treatment attenuates pulmonary arterial hypertension-induced heart failure.	20061549		x	rat	MCT80		

Yen, et al. <sup>39</sup>	2010	Sildenafil limits monocrotaline-induced pulmonary hypertension in rats through suppression of pulmonary vascular remodeling.	20224427	x		rat	MCT60	
Piao, et al. <sup>40</sup>	2010	The inhibition of pyruvate dehydrogenase kinase improves impaired cardiac function and electrical remodeling in two models of right ventricular hypertrophy: resuscitating the hibernating right ventricle.	19949938	x		rat	MCT60 & PAB	x
Drake, et al. <sup>41</sup>	2011	Molecular signature of a right heart failure program in chronic severe pulmonary hypertension.	21719795	x		rat	PAB + Suhx +Cu2diet	
Saini-Chohan, et al. <sup>42</sup>	2011	Persistent pulmonary hypertension results in reduced tetralinoleoyl-cardiolipin and mitochondrial complex II + III during the development of right ventricular hypertrophy in the neonatal pig heart.	21841017	x		piglet	hypoxia	
Baandrup, et al. <sup>43</sup>	2011	Pressure load: the main factor for altered gene expression in right ventricular hypertrophy in chronic hypoxic rats.	21246034	x		rat	hypoxia + PAB	
Bokhari, et al. <sup>44</sup>	2011	PET imaging may provide a novel biomarker and understanding of right ventricular dysfunction in patients with idiopathic pulmonary arterial hypertension.	21926260		x			iPAH
Wong, et al. <sup>45</sup>	2011	Right ventricular failure in idiopathic pulmonary arterial hypertension is associated with inefficient myocardial oxygen utilization.	21900188		x			iPAH
Wong, et al. <sup>46</sup>	2011	Systolic pulmonary artery pressure and heart rate are main determinants of oxygen consumption in the right ventricular myocardium of patients with idiopathic pulmonary arterial hypertension.	22016028		x			iPAH



Qipshidze, et al. <sup>47</sup>	2012	Autophagy mechanism of right ventricular remodeling in murine model of pulmonary artery constriction.	22101525		x	mouse	PAB	
Mosele, et al. <sup>48</sup>	2012	Effects of purple grape juice in the redox-sensitive modulation of right ventricular remodeling in a pulmonary arterial hypertension model.	22441302		x	rat	MCT60	
Khoo, et al. <sup>49</sup>	2012	Obesity-induced tissue free radical generation: an in vivo immuno-spin trapping study.	22564528		x	mouse	Diet + DMPO + MCT60	
Fang, et al. <sup>50</sup>	2012	Therapeutic inhibition of fatty acid oxidation in right ventricular hypertrophy: exploiting Randle's cycle.	21874543		x	rat	PAB	x
Fang, et al. <sup>51</sup>	2012	Comparison of 18F-FDG uptake by right ventricular myocardium in idiopathic pulmonary arterial hypertension and pulmonary arterial hypertension associated with congenital heart disease.	23130105					iPAH vs. CHD-PAH
Wong, et al. <sup>52</sup>	2013	11C-Acetate clearance as an index of oxygen consumption of the right myocardium in idiopathic pulmonary arterial hypertension: a validation study using 15O-labeled tracers and PET.	23735834					iPAH
Sutendra, et al. <sup>53</sup>	2013	A metabolic remodeling in right ventricular hypertrophy is associated with decreased angiogenesis and a transition from a compensated to a decompensated state in pulmonary hypertension.	23846254		x	rat	MCT	x
Piao, et al. <sup>54</sup>	2013	Cardiac glutaminolysis: a maladaptive cancer metabolism pathway in the right ventricle in pulmonary hypertension.	23794090		x	rat	PAB & MCT60	x
Drake, et al. <sup>55</sup>	2013	Chronic carvedilol treatment partially reverses the right ventricular failure transcriptional profile in experimental pulmonary hypertension.	23632417	2013387359	x	rat	SuHx	
Alzoubi, et al. <sup>56</sup>	2013	Dehydroepiandrosterone restores right ventricular structure and function in rats	23585128		x	rat	SuHx	

Piao, et al. <sup>57</sup>	2013	with severe pulmonary arterial hypertension. FOXO1-mediated upregulation of pyruvate dehydrogenase kinase-4 (PDK4) decreases glucose oxidation and impairs right ventricular function in pulmonary hypertension: therapeutic benefits of dichloroacetate.	23247844		x	x	rat	FHR	PAH	x
Gomez-Arroyo, et al. <sup>58</sup>	2013	Metabolic gene remodeling and mitochondrial dysfunction in failing right ventricular hypertrophy secondary to pulmonary arterial hypertension.	23152488		x	x	rat	SuHx & PAB	PAH	x
Friehs, et al. <sup>59</sup>	2013	Pressure-overload hypertrophy of the developing heart reveals activation of divergent gene and protein pathways in the left and right ventricular myocardium.	23262132		x		rabbit	PAB		
Enache, et al. <sup>60</sup>	2013	Skeletal muscle mitochondrial dysfunction precedes right ventricular impairment in experimental pulmonary hypertension.	23099843		x		rat	MCT60		x
Kojonazarov, et al. <sup>61</sup>	2013	The peroxisome proliferator-activated receptor $\beta/\delta$ agonist GW0742 has direct protective effects on right heart hypertrophy.	25006409		x		mice	PAB		
Yoshinaga, et al. <sup>62</sup>	2013	Attenuated right ventricular energetics evaluated using $^{13}\text{C}$ -acetate PET in patients with pulmonary hypertension.	24615469			x			PH	
Wang, et al. <sup>63</sup>	2013	Evaluation of right ventricular volume and ejection fraction by gated (18)F-FDG PET in patients with pulmonary hypertension: comparison with cardiac MRI and CT.	23354658			x			PH	
Lundgrin, et al. <sup>64</sup>	2013	Fasting 2-deoxy-2-[18F]fluoro-D-glucose positron emission tomography to detect metabolic changes in pulmonary arterial hypertension hearts over 1 year.	23509326			x			PAH	
Ikeda, et al. <sup>65</sup>	2014	Crucial role of rho-kinase in pressure overload-induced right ventricular hypertrophy and dysfunction in mice.	24675663	2014358537	x		mouse	PAB		

Hemnes, et al. <sup>66</sup>	2014	Evidence for right ventricular lipotoxicity in heritable pulmonary arterial hypertension.	24274756	x	mouse	BMPR2 & PAB	
Rawat, et al. <sup>67</sup>	2014	Increased reactive oxygen species, metabolic maladaptation, and autophagy contribute to pulmonary arterial hypertension-induced ventricular hypertrophy and diastolic heart failure.	25267798	x	rat	SuHx	
Liu, et al. <sup>68</sup>	2014	Inhibition of NOX/VPO1 pathway and inflammatory reaction by trimethoxystilbene in prevention of cardiovascular remodeling in hypoxia-induced pulmonary hypertensive rats.	24492474	x	rat	hypoxia	
Ahmed, et al. <sup>69</sup>	2014	Naringenin adds to the protective effect of L-arginine in monocrotaline-induced pulmonary hypertension in rats: favorable modulation of oxidative stress, inflammation and nitric oxide.	24878387	x	rat	MCT60	
Frazziano, et al. <sup>70</sup>	2014	Nox-derived ROS are acutely activated in pressure overload pulmonary hypertension: indications for a seminal role for mitochondrial Nox4.	24213612	x	mouse	PAC + Nox2 <sup>-/-</sup> , p47phox <sup>-/-</sup>	
Nergui, et al. <sup>71</sup>	2014	Role of endothelial nitric oxide synthase and collagen metabolism in right ventricular remodeling due to pulmonary hypertension.	24705390	x	mice	hypoxia + eNOS <sup>-/-</sup>	
Ahmed, et al. <sup>72</sup>	2014	Role of oxidative stress, inflammation, nitric oxide and transforming growth factor-beta in the protective effect of diosgenin in monocrotaline-induced pulmonary hypertension in rats.	25062790	x	rat	MCT60	
Zhang, et al. <sup>73</sup>	2014	Up-regulation of hexokinase1 in the right ventricle of monocrotaline induced pulmonary hypertension.	25287584	x	rat	MCT50	x
Tatebe, et al. <sup>74</sup>	2014	Enhanced [18F]fluorodeoxyglucose accumulation in the right ventricular free wall predicts long-term prognosis of	24408936				x
							PAH

Yang, et al. <sup>75</sup>	2014	patients with pulmonary hypertension: a preliminary observational study. The ratio of (18)F-FDG activity uptake between the right and left ventricle in patients with pulmonary hypertension correlates with the right ventricular function.	24662662		x				PH
Paulin, et al. <sup>76</sup>	2015	A miR-208-Mef2 axis drives the decompensation of right ventricular function in pulmonary hypertension.	25287062		x	rat	MCT		x
Moreira-Goncalves, et al. <sup>77</sup>	2015	Cardioprotective effects of early and late aerobic exercise training in experimental pulmonary arterial hypertension.	26463598	2015442750	x	rat	MCT60		
Borgdorff, et al. <sup>78</sup>	2015	Clinical symptoms of right ventricular failure in experimental chronic pressure load are associated with progressive diastolic dysfunction	25486580	2014633325	x	rat	PAB		x
Balestra, et al. <sup>79</sup>	2015	Increased in vivo mitochondrial oxygenation with right ventricular failure induced by pulmonary arterial hypertension: mitochondrial inhibition as driver of cardiac failure?	25645252		x	rat	MCT30 & 60		x
Bruns, et al. <sup>80</sup>	2015	Mitochondrial integrity in a neonatal bovine model of right ventricular dysfunction.	25416385		x	calve	hypoxia		x
Kaur, et al. <sup>81</sup>	2015	Poly (ADP-ribose) polymerase-1: an emerging target in right ventricle dysfunction associated with pulmonary hypertension.	25481773		x	rat	MCT60		
Aziz, et al. <sup>82</sup>	2015	Proteomic Profiling of Early Chronic Pulmonary Hypertension: Evidence for Both Adaptive and Maladaptive Pathology.	26246959		x	dog	DMCT		
Graham, et al. <sup>83</sup>	2015	Severe pulmonary hypertension is associated with altered right ventricle metabolic substrate uptake.	26115672		x	rat	SuHx		x

Khan, et al. <sup>84</sup>	2015	Effects of ranolazine on exercise capacity, right ventricular indices, and hemodynamic characteristics in pulmonary arterial hypertension: a pilot study.	26401256							x		PAH
Sakao, et al. <sup>85</sup>	2015	Increased Right Ventricular Fatty Acid Accumulation in Chronic Thromboembolic Pulmonary Hypertension.	26356218							x		CTEPH
Li, et al. <sup>86</sup>	2015	The Prognostic Value of 18F-FDG Uptake Ratio Between the Right and Left Ventricles in Idiopathic Pulmonary Arterial Hypertension.	26359560	2015437729						x		iPAH
Drozd, et al. <sup>87</sup>	2016	Effects of an endothelin receptor antagonist, Macitentan, on right ventricular substrate utilization and function in a Sugen 5416/hypoxia rat model of severe pulmonary arterial hypertension.	27688036	20160703317	x		rat	SuHx				x
Brittain, et al. <sup>88</sup>	2016	Fatty Acid Metabolic Defects and Right Ventricular Lipotoxicity in Human Pulmonary Arterial Hypertension.	27006481	20160241851	x	x	mouse	BMPR2 R899X				PAH
Talati, et al. <sup>89</sup>	2016	Mechanisms of Lipid Accumulation in the Bone Morphogenetic Protein Receptor Type 2 Mutant Right Ventricle.	27077479				mouse	BMPR2				
Joshi, et al. <sup>90</sup>	2016	MicroRNA-140 is elevated and mitofusin-1 is downregulated in the right ventricle of the Sugen5416/hypoxia/normoxia model of pulmonary arterial hypertension.	27422986				rat	SuHx				
Peters, et al. <sup>91</sup>	2016	Regulation of myoglobin in hypertrophied rat cardiomyocytes in experimental pulmonary hypertension.	27572699				rat	MCT60				
Sun, et al. <sup>92</sup>	2016	Reversal of right ventricular remodeling by dichloroacetate is related to inhibition of mitochondria-dependent apoptosis.	26763846	20160371500	x		rat	MCT60				x
Van der Bruggen, et al. <sup>93</sup>	2016	Bone Morphogenetic Protein Receptor Type 2 Mutation in Pulmonary Arterial Hypertension: A View on the Right	26984938							x		BMPR2 x

		Ventricle.							
Gupte, et al. <sup>94</sup>	2016	Differential Mitochondrial Function in Remodeled Right and Nonremodeled Left Ventricles in Pulmonary Hypertension.	26370778					x	PH
Wang, et al. <sup>95</sup>	2016	Quantitative assessment of right ventricular glucose metabolism in idiopathic pulmonary arterial hypertension patients: a longitudinal study.	26588985	20160851284				x	iPAH x
Sakao, et al. <sup>96</sup>	2016	Right ventricular sugars and fats in chronic thromboembolic pulmonary hypertension.	27323340	20160461412				x	CTEPH
Ohira, et al. <sup>97</sup>	2016	Shifts in myocardial fatty acid and glucose metabolism in pulmonary arterial hypertension: a potential mechanism for a maladaptive right ventricular response.	26060207					x	PAH
Frille, et al. <sup>98</sup>	2016	Thoracic [ <sup>18</sup> F]fluorodeoxyglucose uptake measured by positron emission tomography/computed tomography in pulmonary hypertension.	27336898	20160485669				x	PH
Campos, et al. <sup>99</sup>	2017	Effect of free and nanoencapsulated copaiba oil on monocrotaline-induced pulmonary arterial hypertension.	27798416	20160790386	x	rat	MCT60		
Liu, et al. <sup>100</sup>	2017	Estrogen maintains mitochondrial content and function in the right ventricle of rats with pulmonary hypertension	28320896	20170235187	x	rat	SuHx		x
He, et al. <sup>101</sup>	2017	Galectin-3 mediates the pulmonary arterial hypertension-induced right ventricular remodeling through interacting with NADPH oxidase 4	28431936	20170283180	x	rat	MCT60		
Cowley, et al. <sup>102</sup>	2017	β1A-Subtype Adrenergic Agonist Therapy for Failing Right Ventricle.	28822963		x	mice	bleomycin		
Tian, et al. <sup>103</sup>	2017	Ischemia-induced Drp1 and Fis1-mediated mitochondrial fission and right ventricular dysfunction in pulmonary hypertension	28265681	20170177715	x	rat	MCT60		
Nagy, et al. <sup>104</sup>	2017	Lack of ABCG2 leads to biventricular dysfunction and remodeling in response	28270772	20170166980	x	mice	PAB / hypoxia		

		to hypoxia						
Zhu, et al. <sup>105</sup>	2017	LOX-1 promotes right ventricular hypertrophy in hypoxia-exposed rats	28259654	20170244516	x		rat	hypoxia
Wang, et al. <sup>106</sup>	2017	Oxidative profiling of the failing right heart in rats with pulmonary hypertension.	28472095	20170340497	x		rat	OVA/SuHx
Xu, et al. <sup>107</sup>	2017	PPAR $\gamma$ Alleviates Right Ventricular Failure Secondary to Pulmonary Arterial Hypertension in Rats.	29151490		x		rat	MCT60
Dos Santos Lacerda, et al. <sup>108</sup>	2017	Pterostilbene reduces oxidative stress, prevents hypertrophy and preserves systolic function of right ventricle in cor pulmonale model	28703274	20170659486	x		rat	MCT60
Puukila, et al. <sup>109</sup>	2017	Secoisolariciresinol diglucoside attenuates cardiac hypertrophy and oxidative stress in monocrotaline-induced right heart dysfunction	28321539	20170209991	x		rat	MCT
Saygin, et al. <sup>110</sup>	2017	Metabolic and functional evaluation of the heart and lungs in pulmonary hypertension by gated 2-[18F]-Fluoro-2-deoxy-D-glucose positron emission tomography	28597761	20170459867		x		PH
Siqueira, et al. <sup>111</sup>	2018	Effects of ovariectomy in antioxidant defence systems in right ventricle of female rats with pulmonary arterial hypertension induced by monocrotaline.	28854338		x		rat	MCT

**Table S2. Meta-regression analyses: variables versus duration of RV pressure load.**

	coefficient	constant	std. error	t	P >  t	[95% conf. interval]	
FDG-uptake	-0.006	1.831118	0.028237	-0.21	0.851	-0.12751	0.115473
GLUT1 mRNA	0.007318	1.338181	0.017441	0.42	0.681	-0.03009	0.044725
GLUT1 protein	-0.06177	5.544784	0.193256	-0.32	0.780	-0.89329	0.769742
GLUT4 mRNA	-0.08868	-0.1779	0.094733	-0.94	0.385	-0.32048	0.143124
GLUT4 protein	0.062796	-1.92728	0.044244	1.42	0.251	-0.07801	0.2036
HK1 mRNA	-0.41346	20.52151	0.203145	-2.04	0.081	-0.89382	0.066904
HK2 mRNA	0.013838	-0.26506	0.035005	0.4	0.703	-0.06688	0.09456
CTP1B mRNA	-0.26705	9.571756	0.071064	-3.76	<b>0.033</b>	-0.49321	-0.0409
mitochondrial content	-0.0066	-0.41463	0.009553	-0.69	0.507	-0.02821	0.015005
<i>mitochondrial content (first six weeks only)</i>	<i>-0.12221</i>	<i>2.461455</i>	<i>0.025414</i>	<i>-4.81</i>	<b>0.002</b>	<i>-0.1823</i>	<i>-0.06211</i>
PDH mRNA	-0.0066	-0.26024	0.071658	-0.09	0.935	-0.31492	0.301721
PDK4 mRNA	-0.20665	0.005799	0.178042	-1.16	0.310	-0.70097	0.287676
PGC1a mRNA	-0.06271	0.634076	0.021666	-2.89	<b>0.044</b>	-0.12287	-0.00256
PGC1a protein	-0.04477	0.977281	0.03338	-1.34	0.272	-0.151	0.061461
PPAR mRNA	-0.03096	0.785598	0.023265	-1.33	0.232	-0.0878866	0.025968
MCAD mRNA	-0.10478	-3.09365	0.096481	-1.09	0.313	-0.33292	0.123366
MCAD protein	0.120205	-5.58791	0.080062	1.5	0.272	-0.22427	0.464684
resp. cap. Glucose - ADP driven	-0.00781	-0.53042	0.009609	-0.81	0.566	-0.1299	0.114282
resp. cap. Glucose - whole cells	-0.11876	3.300385	0.114537	-1.04	0.409	-0.61157	0.374057
resp. cap. FA - ADP driven	-0.00753	-0.49098	0.010332	-0.73	0.519	-0.04041	0.025351

Significant p-values shown in **bold**.



**Table S3. Meta-regression analyses: variables versus degree of RV pressure load.**

	coefficient	constant	std. error	t	P >  t	[95% conf. interval]	
FDG-uptake	-0.605857	3.8261	1.127987	-0.54	0.628	-4.19562	2.983902
GLUT1 mRNA	-0.097231	1.875722	0.258773	-0.38	0.771	-3.38525	3.19079
GLUT4 protein	0.6982679	-0.7738904	0.884316	0.79	0.460	-1.46558	2.86211
HK1 mRNA	2.672385	-14.20094	1.530079	1.75	0.223	-3.91101	9.255784
HK2 mRNA	0.2727004	-2.639479	0.392468	0.69	0.518	-0.73617	1.281572
mitochondrial content	-0.490853	0.6067835	0.163592	-3	<b>0.040</b>	-0.94506	-0.03665
PDH mRNA	-0.19941	1.375868	0.195707	-1.02	0.415	-1.04147	0.642648
PDK4 protein	-5.779816	6.268431	8.17396	-0.71	0.608	-109.64	98.0802
PDK1 mRNA	0.2356872	-2.020017	0.125199	1.88	0.311	-1.35512	1.826494
PDK1 protein	1.077672	-0.6647883	2.190228	0.49	0.709	-26.7518	28.90716
MCAD mRNA	1.856523	-19.68273	5.871176	0.32	0.782	-23.4051	27.11816
MCAD protein	-0.287837	0.7897496	0.113183	-2.54	0.239	-1.72596	1.150285
resp. cap. Glucose - ADP driven	0.2589947	-1.225371	0.286097	0.91	0.432	-0.65149	1.169482
resp. cap. FA - ADP driven	-0.257863	0.0167995	0.519064	-0.5	0.669	-2.49122	1.975488

Significant p-values shown in **bold**.

**Table S4. Level of significance of meta-analysis and meta-regression.**

parameter	<i>mRNA expression level</i>				<i>protein expression level</i>			
	meta-analysis	model effect (increased compared)	duration effect	effect of degree of pressure load	meta-analysis	model effect (increased compared)	duration effect	effect of degree of pressure load
GLUT1	↑ (0.000)	~	~	~	↑ (0.009)	MCT vs. hypoxia, PAB and FHR	~	~
GLUT4	~	~	~	~	~	~	~	~
CTP1B	~	~	↓ (0.033)	N/A	N/A	N/A	N/A	N/A
HK1	↑ (0.000)	~	↘ (0.081)	~	N/A	N/A	N/A	N/A
HK2	~	~	~	~	N/A	N/A	N/A	N/A
PDH	~	~	~	~	↘ (0.123)	~	~	N/A
PDK4	↘ (0.110)	~	~	~	~	~	N/A	-
PDK1	N/A	N/A	N/A	~	~	~	N/A	~
PDK2	N/A	N/A	N/A	N/A	~	~	N/A	N/A
MCAD	↓ (0.000)	~	~	~	↘ (0.141)	~	~	~
PGC1α	↓ (0.008)	~	↓ (0.044)	~	~	MCT vs. SuHx	~	N/A
PPARα	~	~	~	N/A	N/A	N/A	N/A	N/A

<i>in vivo measurements</i>				
parameter	meta-analysis	model effect (increased compared)	duration effect	effect of degree of pressure load
FDG-uptake	↑ (0.000)	~	~	~
Glycolysis – whole cells (i.e. Langendorf, Seahorse)	↑ (0.000)	~	N/A	N/A
Respiratory capacity, carbohydrates – isolated mitochondria (i.e. Oroboros, Clark-type)	↘ (0.085)	~	~	~
Respiratory capacity, carbohydrates – whole cells (i.e. Langendorf, Seahorse)	↘ (0.082)	MCT vs. PAB and FHR	~	N/A
Respiratory capacity, fatty acids – isolated mitochondria (i.e. Oroboros, Clark-type)	↓ (0.001)	~	↘ (0.130)	~
Respiratory capacity, fatty acids – whole cells (i.e. Langendorf, Seahorse)	~	PAB vs. SuHx.	N/A	N/A

<i>combined measurements</i>				
parameter	meta-analysis	model effect	duration effect	effect of degree of pressure load
Mitochondrial content	~	~	~	~
			(≤6 days (0.002))	

↑ significant increase or positive relation; ↓ significant decrease or negative relation; ↗ positive trend ( $p < 0.15$ ); ↘ negative trend ( $p < 0.15$ ); ~ unchanged.

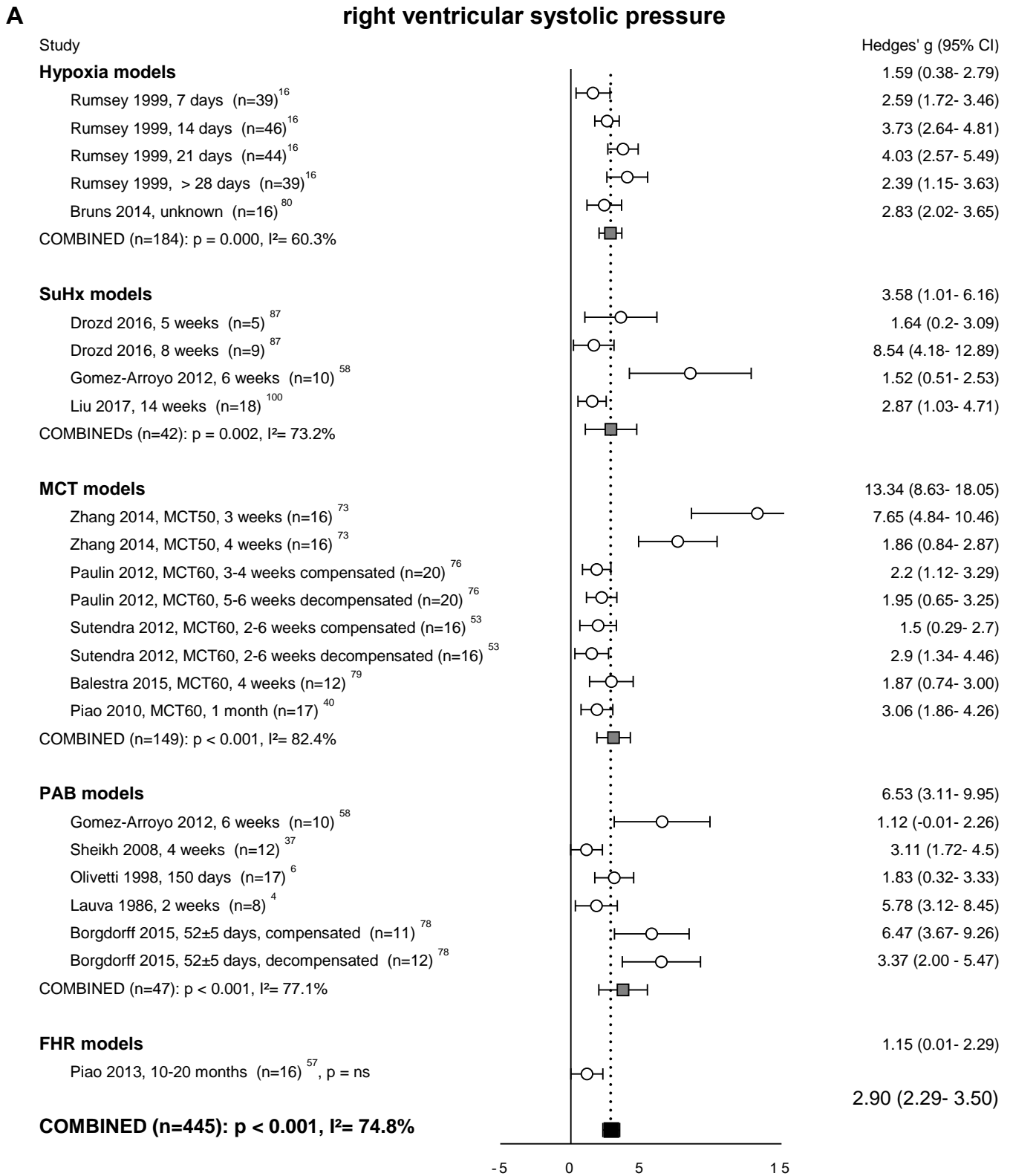
**Table S5. Overview of Hedges' g for metabolic parameters in models of RV pressure load subjected to therapeutic interventions.**

							Hedges' g																		
animal	#	Year	Author	Hit duration	Model	Therapie	GLUT1 - mRNA	GLUT1 - protein	GLUT4 - protein	FDG-uptake	CPT1B - mRNA	CPT1A - protein	HK1 - mRNA	HK1 - protein	HK2 - mRNA	PDH - activity	PDHa1 - protein	PDK4 - mRNA	PDK4 - protein	PDK1 - mRNA	PDK1 - protein	PDK2 - mRNA	PDK2 - protein	PGC1alpha - protein	
Rat	19949938	2010	Piao <sup>40</sup>	1 month	MCT60	DCA	-1.68	-2.58								-0.99									
Rat	23247844	2012	Piao <sup>57</sup>	10-20 months	FHR	DCA, acute treatment																			
Rat	23247844	2012	Piao <sup>57</sup>	10-20 months	FHR	DCA, chronic treatment (6 months)	-1.44				0.01				-2.74*	4.13*		-1.51*	0.58	0.36	0.48	0.60	-0.95		
Rat	26763846	2016	Sun <sup>92</sup>	6 weeks	MCT	DCA 50mg/kg											1.62*		-6.14*		0.47		-1.78*		
Rat	26763846	2016	Sun <sup>92</sup>	6 weeks	MCT	DCA 150mg/kg											3.27*		-0.86*		0.40		-2.6*		
Rat	26763846	2016	Sun <sup>92</sup>	6 weeks	MCT	DCA 200 mg/kg											3.38*		-6.89*		0.33		-3.20*		
Rat	23794090	2013	Piao <sup>54</sup>	4 weeks	MCT	DON	-2.19									1.14*									
Rat	27688036	2016	Droz <sup>87</sup>	9 weeks	SuHx	ERA			-2.67*	-1.20															
Rat	28320896	2017	Liu <sup>100</sup>	14 weeks	SuHx	oestrogen																		3.36*	
Rat	21874543	2012	Fang <sup>50</sup>	4 weeks	PAB	RAN	-1.46*	-0.45604				-1.83*	-2.55*	-0.46	-0.08	2.01*									
Rat	21874543	2012	Fang <sup>50</sup>	4 weeks	PAB	RAN, in vitro																			
Rat	21874543	2012	Fang <sup>50</sup>	8 weeks	PAB	TMZ	-1.30*	-1.33*				-1.41*	-1.18*	-0.18	-0.18	1.36*									
Rat	21874543	2012	Fang <sup>50</sup>	8 weeks	PAB	TMZ, in vitro																			

							Hedges'g								
animal	#	Year	Author	Hit duration	Model	Therapie	Glycolysis	Mitochondrial resp. capacity Glucose, isolated mitochondria	Mitochondrial resp. capacity Glucose, Langendorf	Mitochondrial resp. capacity Glucose, Seahorse	Mitochondrial resp. capacity fatty acids, isolated mitochondria	Mitochondrial resp. capacity FA, Langendorf	Mitochondrial resp. capacity FA, Seahorse	Mitochondrial content	Fulton
Rat	19949938	2010	Piao <sup>40</sup>	1 month	MCT60	DCA	0.65		3.20*						-1.59*
Rat	23247844	2012	Piao <sup>57</sup>	10-20 months	FHR	DCA, acute treatment	-0.79		3.51*			-1.22*			
Rat	23247844	2012	Piao <sup>57</sup>	10-20 months	FHR	DCA, chronic treatment (6 months)	-0.71			0.35			0.40		
Rat	26763846	2016	Sun <sup>92</sup>	6 weeks	MCT	DCA 50mg/kg									-2.72*
Rat	26763846	2016	Sun <sup>92</sup>	6 weeks	MCT	DCA 150mg/kg									-5.83*
Rat	26763846	2016	Sun <sup>92</sup>	6 weeks	MCT	DCA 200 mg/kg									-5.97*
Rat	23794090	2013	Piao <sup>54</sup>	4 weeks	MCT	DON									-0.92
Rat	27688036	2016	Droz <sup>87</sup>	9 weeks	SuHx	ERA									
Rat	28320896	2017	Liu <sup>100</sup>	14 weeks	SuHx	oestrogen		0.38			0.36			-0.01	-1.01*
Rat	21874543	2012	Fang <sup>50</sup>	4 weeks	PAB	RAN	-0.99			2.98*		-1.34*			-2.16*
Rat	21874543	2012	Fang <sup>50</sup>	4 weeks	PAB	RAN, in vitro						-14.63*			
Rat	21874543	2012	Fang <sup>50</sup>	8 weeks	PAB	TMZ	-1.47*		2.43 * (10 mM gluc), 1.99* (5mM gluc).			-1.28*	-7.29*		-1.79*
Rat	21874543	2012	Fang <sup>50</sup>	8 weeks	PAB	TMZ, in vitro						-4.18*			

\* p mentioned in study < 0.05

**Figure S1. Models of increased pressure load.**



**B**

**Fulton index**

Study

Hedges' g (95% CI)

**Hypoxia models**

- Adroque 2005, 4 weeks (n=10)<sup>25</sup>
- Adroque 2005, 10 weeks (n=10)<sup>25</sup>
- Adroque 2005, 12 weeks (n=10)<sup>25</sup>
- Sharma 2003, 2 days (n=10)<sup>23</sup>
- Sharma 2003, 7 days (n=10)<sup>23</sup>
- Sharma 2003, 14 days (n=10)<sup>23</sup>
- Nouette-Gaullain 2005, 14 days (n=30)<sup>24</sup>
- Nouette-Gaullain 2005, 21 days (n=30)<sup>24</sup>

COMBINED (n=120): p < 0.001, I<sup>2</sup>= 81.4%

**SuHx models**

- Graham 2015, 7 weeks (n=5)<sup>83</sup>
- Drozd 2016, 8 weeks (n=9)<sup>87</sup>
- Gomez-Arroyo 2012, 6 weeks (n=10)<sup>58</sup>
- Liu 2017, 14 weeks (n=18)<sup>100</sup>

COMBINED (n=42): p < 0.001, I<sup>2</sup>= 62.8%

**MCT models**

- Broderick 2008, MCT60, 46 days (n=67)<sup>35</sup>
- Zhang 2014, MCT50, 3 weeks (n=16)<sup>73</sup>
- Zhang 2014, MCT50, 4 weeks (n=16)<sup>73</sup>
- Enache 2013, MCT60, 2 weeks (n=26)<sup>60</sup>
- Enache 2013, MCT60, 4 weeks compensated (n=17)<sup>60</sup>
- Enache 2013, MCT60, 4 weeks decompensated (n=15)<sup>60</sup>
- Sutendra 2012, MCT60, 2-6 weeks compensated (n=16)<sup>53</sup>
- Sutendra 2012, MCT60, 2-6 weeks decompensated (n=16)<sup>53</sup>
- Balestra 2015, MCT60, 4 weeks (n=12)<sup>79</sup>
- Piao 2010, MCT60, 1 month (n=10.5)<sup>40</sup>
- Piao 2013, MCT60, 4 weeks (n=14)<sup>54</sup>
- Paulin 2015, MCT60, 3-6 weeks, compensated (n=20)<sup>76</sup>
- Paulin 2015, MCT60, 3-6 weeks, decompensated (n=20)<sup>76</sup>
- Sun 2015, MCT50, 6 weeks (n=14)<sup>92</sup>

COMBINED (n=291.5): p < 0.001, I<sup>2</sup>= 86.4%

**PAB models**

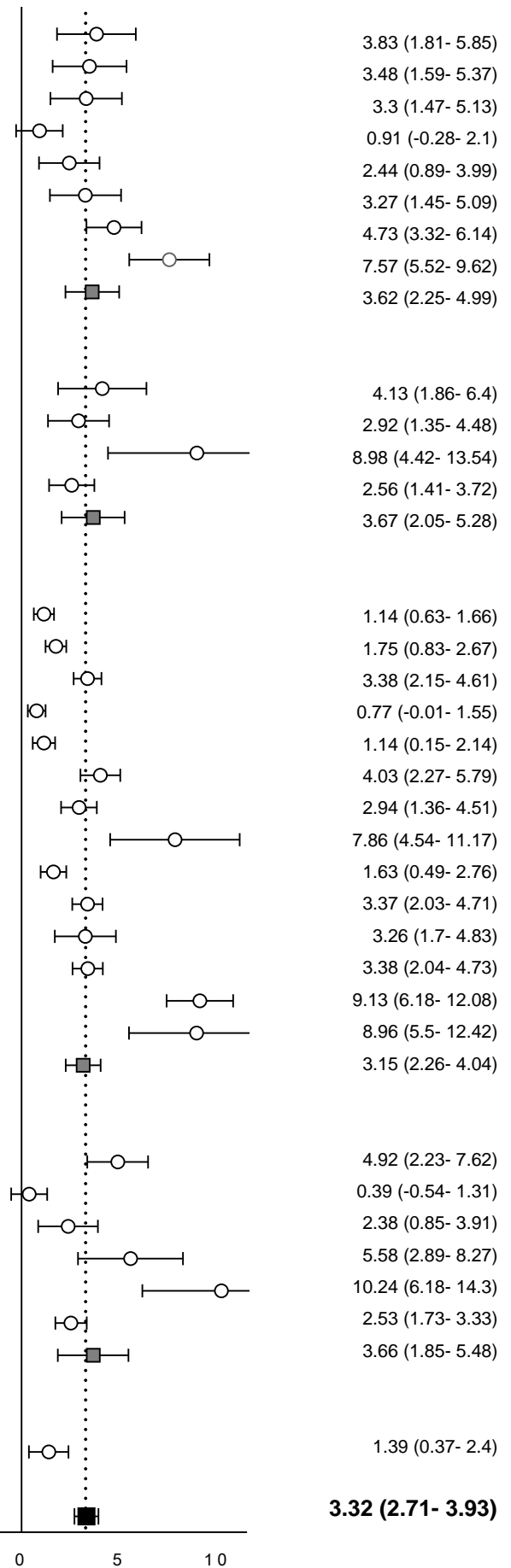
- Gomez-Arroyo 2012, 6 weeks (n=10)<sup>58</sup>
- Olivetti 1998, 150 days (n=17)<sup>6</sup>
- Fang 2012, 8 weeks (n=12)<sup>50</sup>
- Fang 2012, 4 weeks (n=12)<sup>50</sup>
- Piao 2013, 4 weeks (n=13)<sup>54</sup>
- Sack 1997, 7 days (n=43)<sup>14</sup>

COMBINED (n=107): p < 0.001, I<sup>2</sup>= 87.6%

**FHR models**

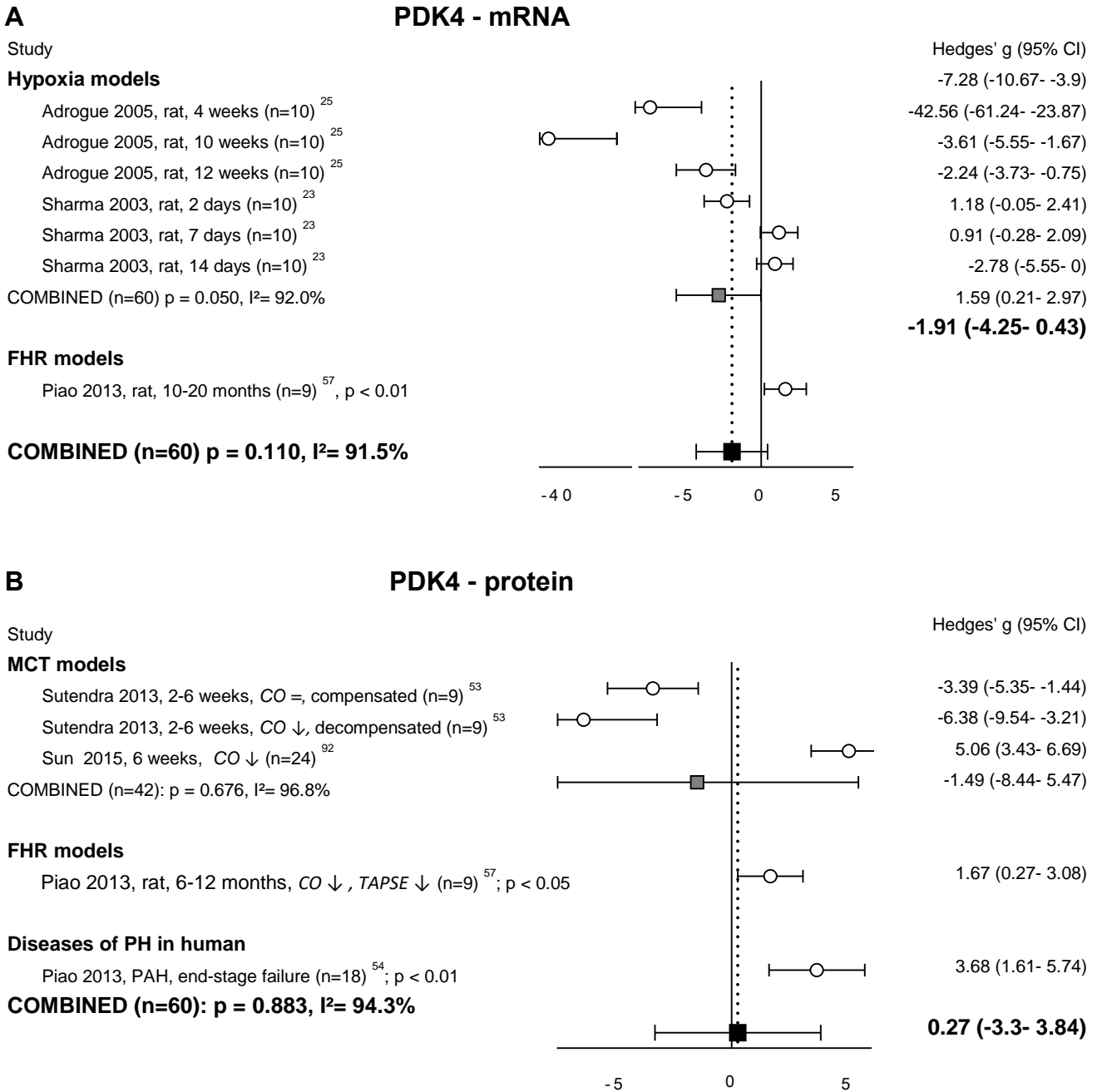
- Piao 2013, 6-12 months (n=16)<sup>57</sup>, p < 0.05

**COMBINED (n=576.5): p < 0.001, I<sup>2</sup>= 84.3%**



Forest plots of right ventricular systolic pressure (A) and Fulton index (B). Data are presented as Hedges'  $g$  (95% confidence interval). Combined Hedges'  $g$  are presented as squares: grey representing Hedges'  $g$  of a specific model, black representing Hedges'  $g$  of all included studies. Bars represent 95% confidence interval. *CI = confidence interval.  $n$  = number of included animals.  $i^2$  = level of heterogeneity.*

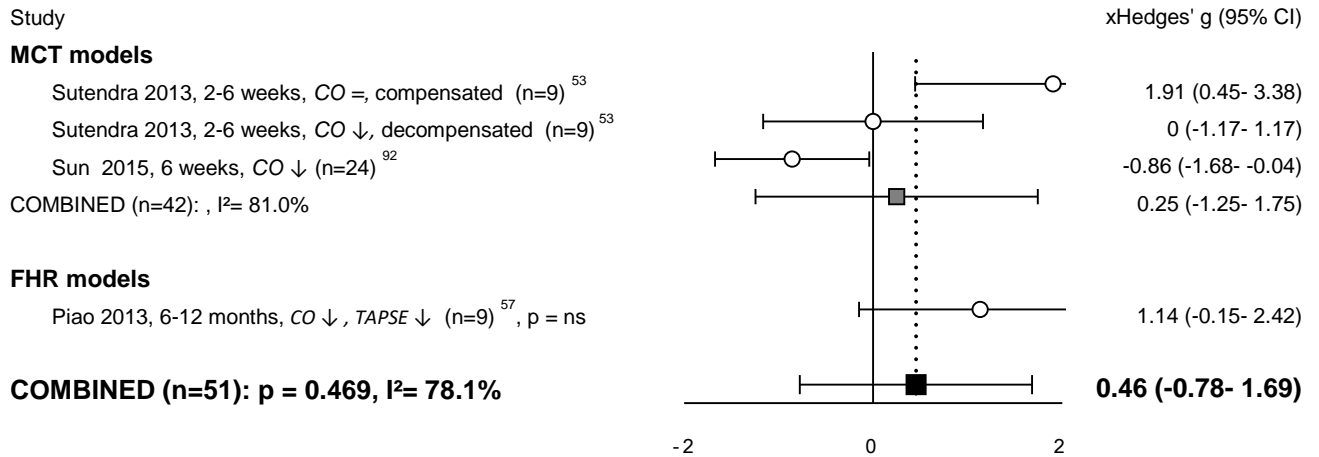
Figure S2. Forest plots of expression of PDK isoenzymes.





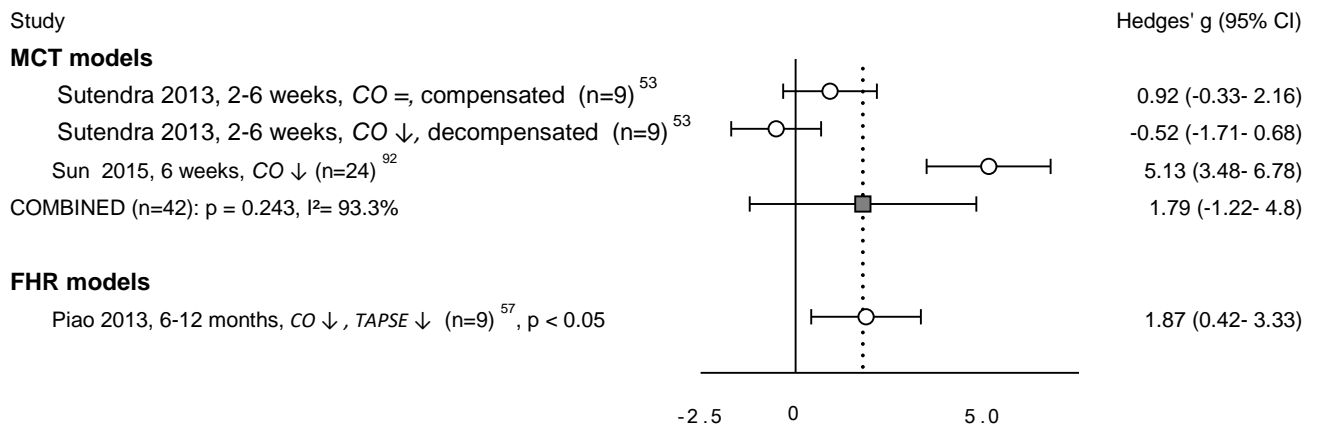
### C

### PDK1 - protein



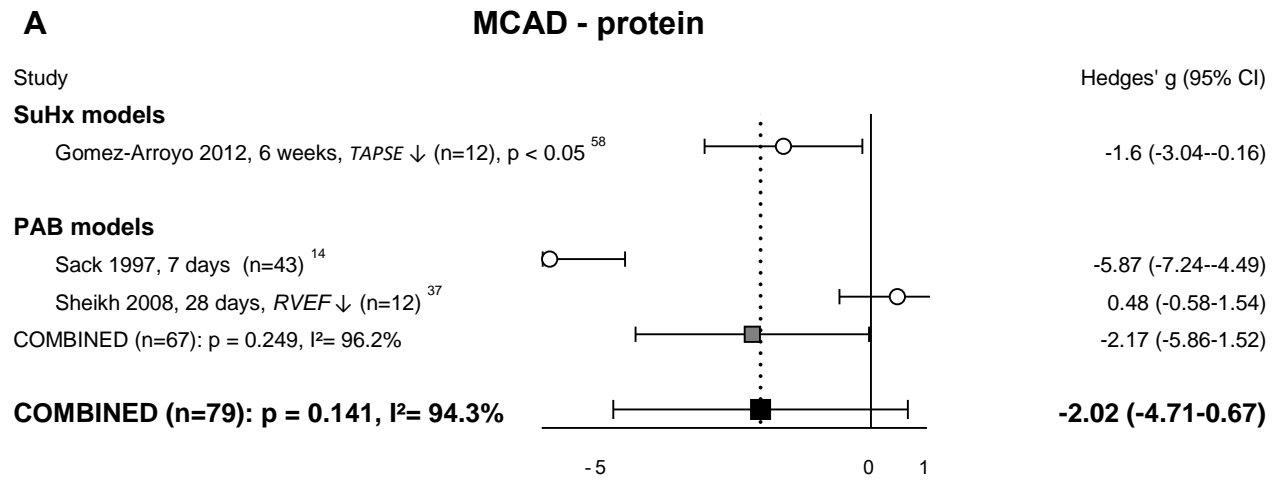
### D

### PDK2 - protein



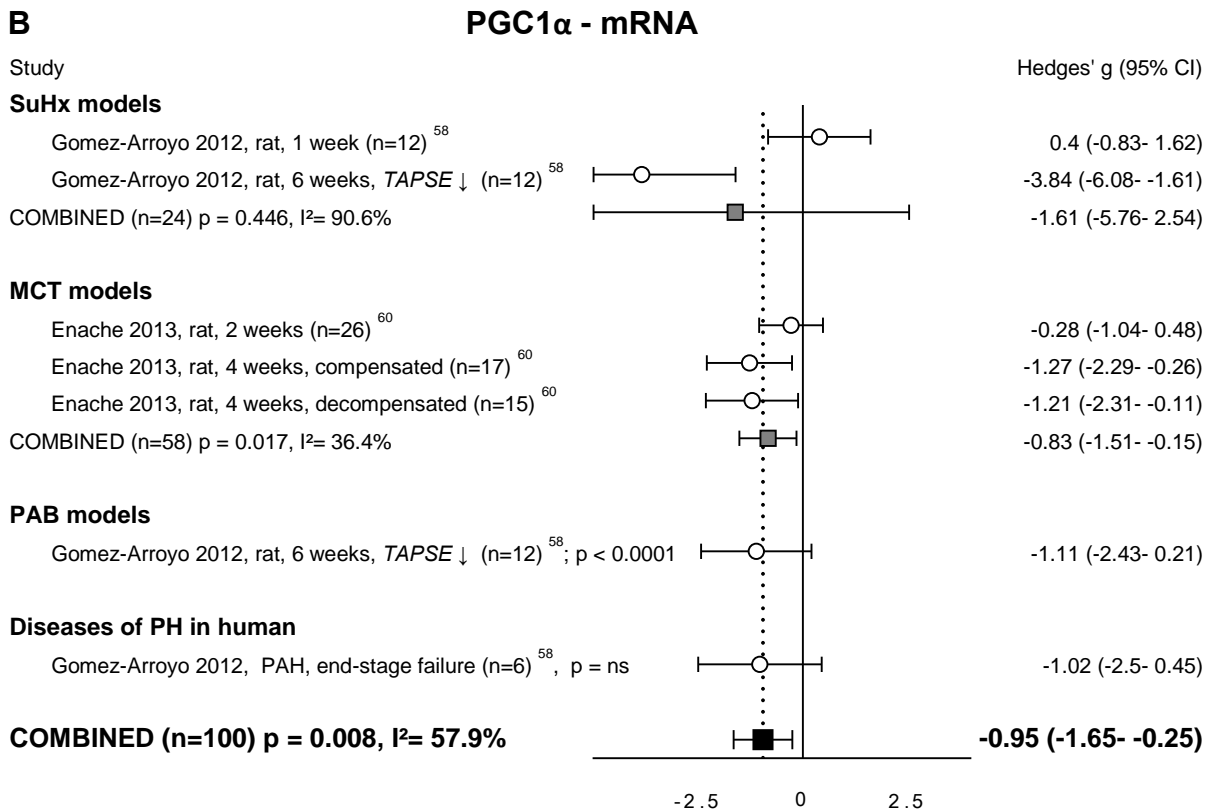
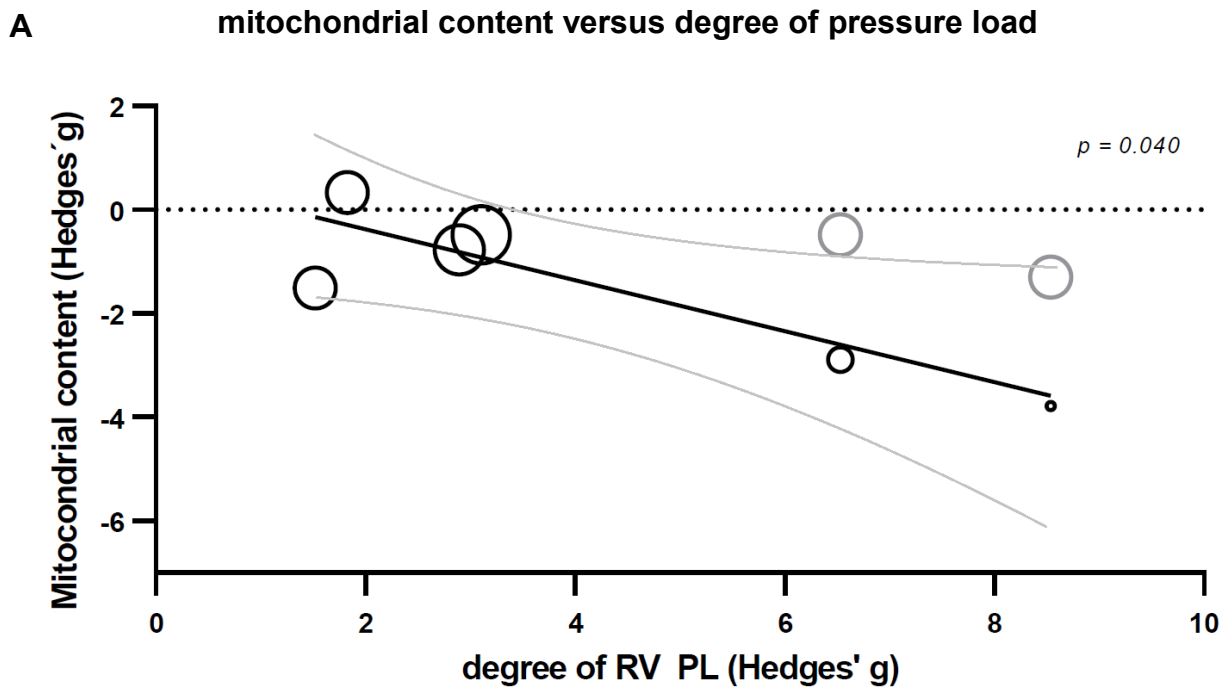
PDK4 at both mRNA (A) and protein level (B), and PDK1 (C) and PDK2 (D) at protein level. Bars represent 95% confidence interval. PDK = pyruvate dehydrogenase kinase. CO = cardiac output, CI = cardiac index, TAPSE = tricuspid annular plane systolic movement, RVEF = RV ejection fraction, ↓ = decreased, “=” = not statistically significant affected. 95% CI = 95% confidence interval, n = number of included animals, I<sup>2</sup> = level of heterogeneity, x = not included in meta-analysis.

**Figure S3. Forest plot MCAD at protein level.**

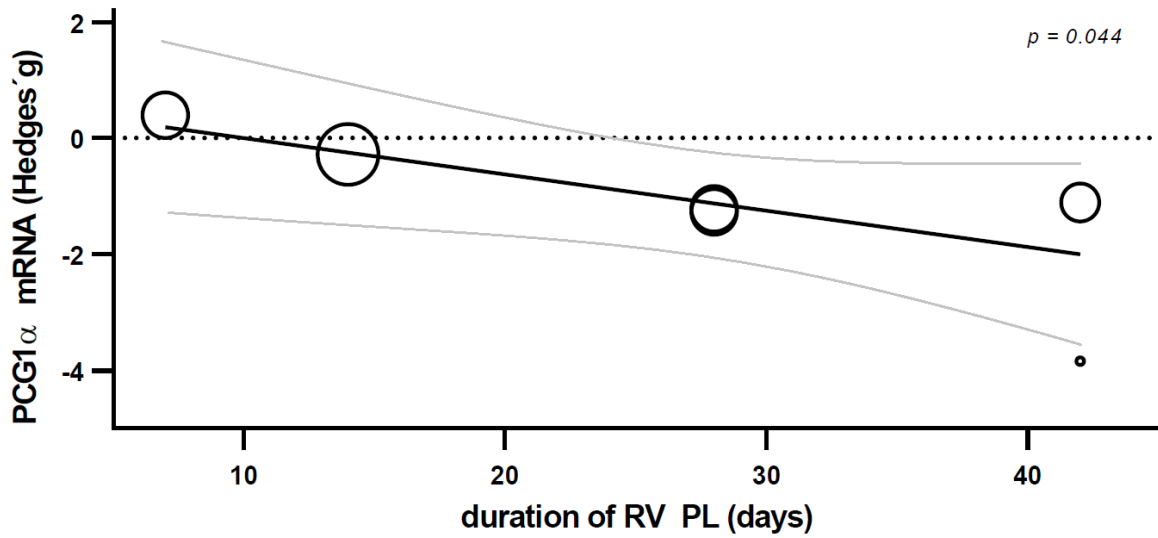


Bars represent 95% confidence interval. MCAD = medium chain acyl CoA dehydrogenase. *CO* = cardiac output, *CI* = cardiac index, *TAPSE* = tricuspid annular plane systolic movement, *RVEF* = RV ejection fraction, ↓ = decreased, “=” = not statistically significant affected. 95% CI = 95% confidence interval, n = number of included animals, *i*<sup>2</sup> = level of heterogeneity, x = not included in meta-analysis.

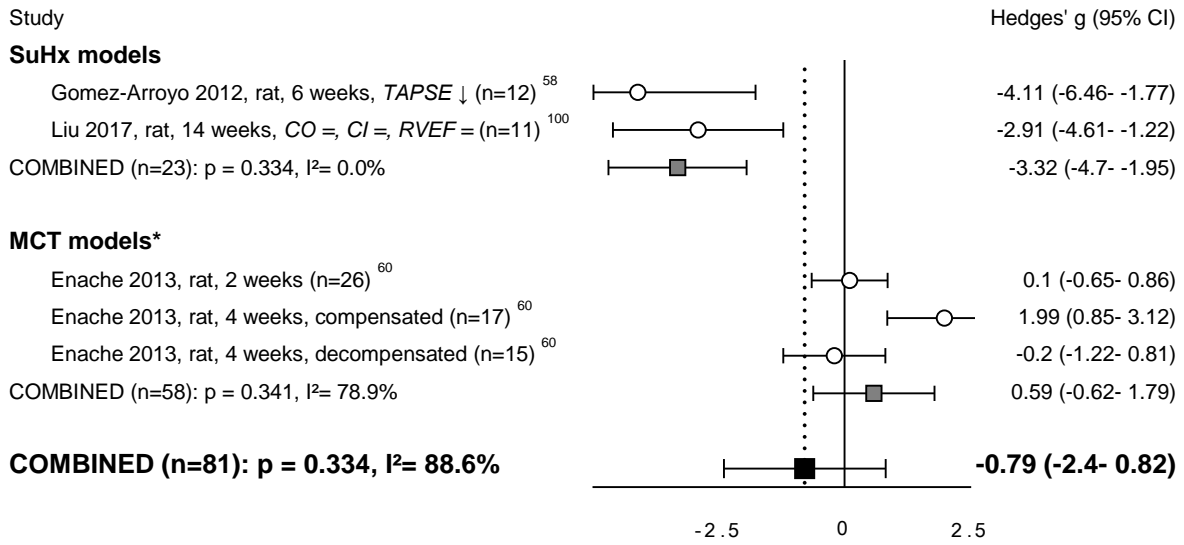
Figure S4. Regulators of metabolism.



**C PGC1 $\alpha$  (mRNA) versus duration of pressure load**

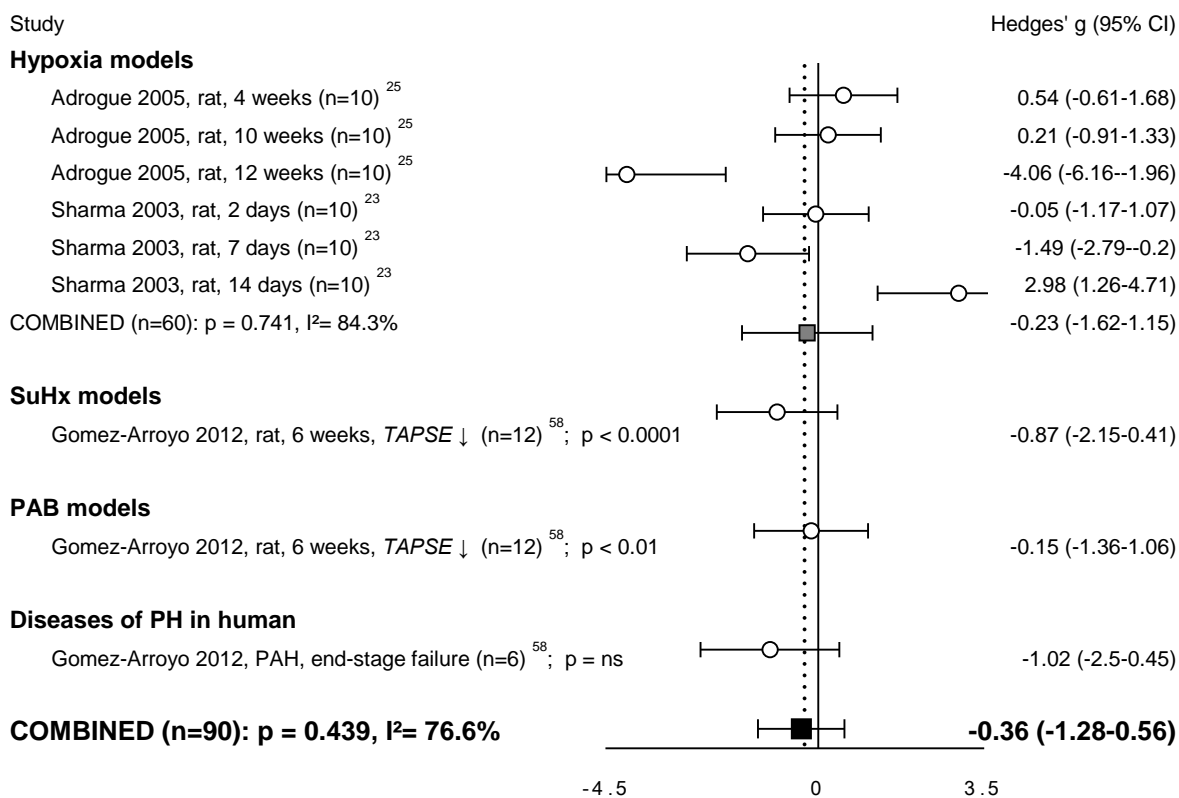


**D PGC1 $\alpha$  - protein**



## E

## PPAR $\alpha$ - mRNA



Meta-regression of mitochondrial content with degree of RV pressure load (A). PGC1 $\alpha$  gene expression(B) and its relation with duration of pressure load shown by meta-regression in a bubble plot (C). Forrest plot of PGC1 $\alpha$  protein expression (D). Forrest plot of PPAR $\alpha$  gene expression (E). Data are presented as Hedges' g. Combined Hedges' g are presented as squares: grey representing Hedges' g of a specific model, black representing Hedges' g of all included studies. Bars represent 95% confidence interval. Bubble size represents relative study precision, calculation based on standard deviation. Black line represents regression line, grey lines represents 95% confidence interval. CO = cardiac output, CI = cardiac index, TAPSE = tricuspid annular plane systolic movement, RVEF = RV ejection fraction,  $\downarrow$  = decreased, "=" = not statistically significant affected. 95% CI = 95% confidence interval, n = number of included animals,  $i^2$  = level of heterogeneity. \* = significantly ( $p < 0.05$ ) increased compared to SuHx-model.

### Supplemental References:

1. Cooper G, Satava RM, Harrison CE, Coleman HN. Normal myocardial function and energetics after reversing pressure overload hypertrophy. *American Journal of Physiology*. 1974;226:1158–1165.
2. Cooper G 4th, Tomanek RJ, Ehrhardt JC, Marcus ML. Chronic progressive pressure overload of the cat right ventricle. *Circulation research*. 1981;48:488–497.
3. Reibel DK, Uboh CE, Kent RL. Altered coenzyme A and carnitine metabolism in pressure-overload hypertrophied hearts. *American Journal of Physiology - Heart and Circulatory Physiology*. 1983;13:H839–H843.
4. Lauva IK, Brody E, Tiger E, Kent RL, Copper G 4th, Marino TA. Control of myocardial tissue components and cardiocyte organelles in pressure-overload hypertrophy of the cat right ventricle. *The American journal of anatomy*. 1986;177:71–80.
5. Schneider M, Wiese S, Kunkel B, Hauk H, Pfeiffer B. Development and regression of right heart ventricular hypertrophy: Biochemical and morphological aspects. *Zeitschrift fur Kardiologie*. 1987;76:1–8.
6. Olivetti G, Ricci R, Lagrasta C, Maniga E, Sonnenblick EH, Anversa P. Cellular basis of wall remodeling in long-term pressure overload-induced right ventricular hypertrophy in rats. *Circulation Research*. 1988;63:648–657.
7. Hung KS, Pacheco H, Lessin D, Jordan K, Mattioli L. Morphometry of right ventricular papillary muscle in rat during development and regression of hypoxia-induced hypertension. *Advances in experimental medicine and biology*. 1988;227:337–346.
8. Saito D, Tani H, Kusachi S, Uchida S, Ohbayashi N, Marutani M, Maekawa K, Tsuji T, Haraoka S. Oxygen metabolism of the hypertrophic right ventricle in open chest dogs. *Cardiovascular Research*. 1991;25:731–736.
9. Morioka S, Honda M, Ishikawa S, Ishinaga Y, Yano S, Tanaka K, Moriyama K. Changes in contractile and non-contractile proteins, intracellular Ca<sup>2+</sup> and ultrastructures during the development of right ventricular hypertrophy and failure in rats. *Japanese Circulation Journal*. 1992;56:469–474.
10. Sivitz WI, Lund DD, Yorek B, Grover-McKay M, Schmid PG. Pretranslational regulation of two cardiac glucose transporters in rats exposed to hypobaric hypoxia. *American Journal of Physiology - Endocrinology and Metabolism*. 1992;263:E562–E569.
11. Baudet S, Kuznetsov A, Merciai N, Gorza L, Ventura-Clapier R. Biochemical, mechanical and energetic characterization of right ventricular hypertrophy in the ferret heart. *Journal of Molecular and Cellular Cardiology*. 1994;26:1573–1586.
12. Ishikawa K, Hashimoto H, Mitani S, Toki Y, Okumura K, Ito T. Enalapril improves heart failure induced by monocrotaline without reducing pulmonary hypertension in rats: Roles of

preserved myocardial creatine kinase and lactate dehydrogenase isoenzymes. *International Journal of Cardiology*. 1995;47:225–233.

13. Do E, Baudet S, Gow IF, Ellis D, Noireaud J. Intracellular pH during hypoxia in normal and hypertrophied right ventricle of ferret heart. *Journal of Molecular and Cellular Cardiology*. 1995;27:927–939.
14. Sack MN, Disch DL, Rockman HA, Kelly DP. A role for Sp and nuclear receptor transcription factors in a cardiac hypertrophic growth program. *Proceedings of the National Academy of Sciences of the United States of America*. 1997;94:6438–6443.
15. Nagaya N, Goto Y, Satoh T, Uematsu M, Hamada S, Kuribayashi S, Okano Y, Kyotani S, Shimotsu Y, Fukuchi K, Nakanishi N, Takamiya M, Ishida Y. Impaired regional fatty acid uptake and systolic dysfunction in hypertrophied right ventricle. *Journal of Nuclear Medicine*. 1998;39:1676–1680.
16. Rumsey WL, Abbott B, Bertelsen D, Mallamaci M, Hagan K, Nelson D, Erecinska M. Adaptation to hypoxia alters energy metabolism in rat heart. *American Journal of Physiology - Heart and Circulatory Physiology*. 1999;276:H71–H80.
17. O'Brien TX, Schuyler GT, Rackley MS, Thompson JT. F1 ATP synthase  $\beta$ -subunit and cytochrome c transcriptional regulation in right ventricular hemodynamic overload and hypertrophically stimulated cardiocytes. *Journal of Molecular and Cellular Cardiology*. 1999;31:167–178.
18. Matsushita T, Ikeda S, Miyahara Y, Yakabe K, Yamaguchi K, Furukawa K, Iwasaki T, Shikuwa M, Fukui J, Kohno S. Use of [123I]-BMIPP myocardial scintigraphy for the clinical evaluation of a fatty-acid metabolism disorder of the right ventricle in chronic respiratory and pulmonary vascular disease. *Journal of International Medical Research*. 2000;28:111–123.
19. Bitar FF, Bitar H, El Sabban M, Nasser M, Yunis KA, Tawil A, Dbaibo GS. Modulation of ceramide content and lack of apoptosis in the chronically hypoxic neonatal rat heart. *Pediatric Research*. 2002;51:144–149.
20. Ecartot-Laubriet A, Rochette L, Vergely C, Sicard P, Teyssier J-R. The Activation Pattern of the Antioxidant Enzymes in the Right Ventricle of Rat in Response to Pressure Overload is of Heart Failure Type. *Heart Disease*. 2003;5:308–312.
21. Farahmand F, Hill MF, Singal PK. Antioxidant and oxidative stress changes in experimental cor pulmonale. *Molecular and Cellular Biochemistry*. 2004;260:21–29.
22. Cisar CR, Balog JM, Anthony NB, Iqbal M, Bottje WG, Donoghue AM. Differential expression of mitochondrial electron transport chain proteins in cardiac tissues of broilers from pulmonary hypertension syndrome-resistant and -susceptible lines. *Poultry Science*. 2004;83:1420–1426.
23. Sharma S, Taegtmeier H, Adroque J, Razeghi P, Sen S, Ngumbela K, Essop MF. Dynamic changes of gene expression in hypoxia-induced right ventricular hypertrophy. *American Journal of Physiology - Heart and Circulatory Physiology*. 2004;286:H1185–H1192.
24. Nouette-Gaulain K, Malgat M, Rocher C, Savineau J-P, Marthan R, Mazat J-P, Sztark F. Time

course of differential mitochondrial energy metabolism adaptation to chronic hypoxia in right and left ventricles. *Cardiovascular Research*. 2005;66:132–140.

25. Adroque J V, Sharma S, Ngumbela K, Essop MF, Taegtmeyer H. Acclimatization to chronic hypobaric hypoxia is associated with a differential transcriptional profile between the right and left ventricle. *Molecular and Cellular Biochemistry*. 2005;278:71–78.
26. Van Beek-Harmsen BJ, Van Der Laarse WJ. Immunohistochemical determination of cytosolic cytochrome c concentration in cardiomyocytes. *Journal of Histochemistry and Cytochemistry*. 2005;53:803–807.
27. Schott P, Singer SS, Kögler H, Neddermeier D, Leineweber K, Brodde O-E, Regitz-Zagrosek V, Schmidt B, Dihazi H, Hasenfuss G. Pressure overload and neurohumoral activation differentially affect the myocardial proteome. *Proteomics*. 2005;5:1372–1381.
28. Faber MJ, Dalinghaus M, Lankhuizen IM, Bezstarosti K, Dekkers DHW, Duncker DJ, Helbing WA, Lamers JMJ. Proteomic changes in the pressure overloaded right ventricle after 6 weeks in young rats: Correlations with the degree of hypertrophy. *Proteomics*. 2005;5:2519–2530.
29. Kluge R, Barthel H, Pankau H, Seese A, Schauer J, Wirtz H, Seyfarth H-J, Steinbach J, Sabri O, Winkler J. Different mechanisms for changes in glucose uptake of the right and left ventricular myocardium in pulmonary hypertension. *Journal of Nuclear Medicine*. 2005;46:25–31.
30. Oikawa M, Kagaya Y, Otani H, Sakuma M, Demachi J, Suzuki J, Takahashi T, Nawata J, Ido T, Watanabe J, Shirato K. Increased [18F]fluorodeoxyglucose accumulation in right ventricular free wall in patients with pulmonary hypertension and the effect of epoprostenol. *Journal of the American College of Cardiology*. 2005;45:1849–1855.
31. Redout EM, Wagner MJ, Zuidwijk MJ, Boer C, Musters RJP, van Hardeveld C, Paulus WJ, Simonides WS. Right-ventricular failure is associated with increased mitochondrial complex II activity and production of reactive oxygen species. *Cardiovascular Research*. 2007;75:770–781.
32. Faber MJ, Dalinghaus M, Lankhuizen IM, Bezstarosti K, Verhoeven AJM, Duncker DJ, Helbing WA, Lamers JMJ. Time dependent changes in cytoplasmic proteins of the right ventricle during prolonged pressure overload. *Journal of Molecular and Cellular Cardiology*. 2007;43:197–209.
33. Basu S, Alzeair S, Li G, Dadparvar S, Alavi A. Etiopathologies associated with intercostal muscle hypermetabolism and prominent right ventricle visualization on 2-deoxy-2[F-18]fluoro-D-glucose-positron emission tomography: significance of an incidental finding and in the setting of a known pulmonary d. *Molecular imaging and biology : MIB : the official publication of the Academy of Molecular Imaging*. 2007;9:333–339.
34. Nagendran J, Gurtu V, Fu DZ, Dyck JRB, Haromy A, Ross DB, Rebeyka IM, Michelakis ED. A dynamic and chamber-specific mitochondrial remodeling in right ventricular hypertrophy can be therapeutically targeted. *Journal of Thoracic and Cardiovascular Surgery*. 2008;136:168-178.e3.
35. Broderick TL, King TM. Upregulation of GLUT-4 in right ventricle of rats with monocrotaline-



induced pulmonary hypertension. *Medical Science Monitor*. 2008;14:BR261–BR264.

36. Mouchaers KTB, Schalij I, Versteilen AMG, Hadi AM, Van Nieuw Amerongen GP, Van Hinsbergh VWM, Postmus PE, Van Der Laarse WJ, Vonk-Noordegraaf A. Endothelin receptor blockade combined with phosphodiesterase-5 inhibition increases right ventricular mitochondrial capacity in pulmonary arterial hypertension. *American Journal of Physiology - Heart and Circulatory Physiology*. 2009;297:H200–H207.
37. Sheikh AM, Barrett C, Villamizar N, Alzate O, Valente AM, Herlong JR, Craig D, Lodge A, Lawson J, Milano C, Jagers J. Right ventricular hypertrophy with early dysfunction: A proteomics study in a neonatal model. *Journal of Thoracic and Cardiovascular Surgery*. 2009;137:1146–1153.
38. Redout EM, Van Der Toorn A, Zuidwijk MJ, Van De Kolk CWA, Van Echteld CJA, Musters RJP, Van Hardeveld C, Paulus WJ, Simonides WS. Antioxidant treatment attenuates pulmonary arterial hypertension-induced heart failure. *American Journal of Physiology - Heart and Circulatory Physiology*. 2010;298:H1038–H1047.
39. Yen C-H, Leu S, Lin Y-C, Kao Y-H, Chang L-T, Chua S, Fu M, Wu C-J, Sun C-K, Yip H-K. Sildenafil limits monocrotaline-induced pulmonary hypertension in rats through suppression of pulmonary vascular remodeling. *Journal of Cardiovascular Pharmacology*. 2010;55:574–584.
40. Piao L, Fang YH, Cadete VJJ, Wietholt C, Urboniene D, Toth PT, Marsboom G, Zhang HJ, Haber I, Rehman J, Lopaschuk GD, Archer SL. The inhibition of pyruvate dehydrogenase kinase improves impaired cardiac function and electrical remodeling in two models of right ventricular hypertrophy: Resuscitating the hibernating right ventricle. *Journal of Molecular Medicine*. 2010;88:47–60.
41. Drake JI, Bogaard HJ, Mizuno S, Clifton B, Xie B, Gao Y, Dumur CI, Fawcett P, Voelkel NF, Natarajan R. Molecular signature of a right heart failure program in chronic severe pulmonary hypertension. *American Journal of Respiratory Cell and Molecular Biology*. 2011;45:1239–1247.
42. Saini-Chohan HK, Dakshinamurti S, Taylor WA, Shen GX, Murphy R, Sparagna GC, Hatch GM. Persistent pulmonary hypertension results in reduced tetralinoleoyl-cardiolipin and mitochondrial complex II + III during the development of right ventricular hypertrophy in the neonatal pig heart. *American Journal of Physiology - Heart and Circulatory Physiology*. 2011;301:H1415–H1424.
43. Baandrup JD, Markvaridsen LH, Peters CD, Schou UK, Jensen JL, Magnusson NE, Ørntoft TF, Kruhøffer M, Simonsen U. Pressure load: The main factor for altered gene expression in right ventricular hypertrophy in chronic hypoxic rats. *PLoS ONE*. 2011;6.
44. Bokhari S, Raina A, Rosenweig EB, Schulze PC, Bokhari J, Einstein AJ, Barst RJ, Johnson LL. PET imaging may provide a novel biomarker and understanding of right ventricular dysfunction in patients with idiopathic pulmonary arterial hypertension. *Circulation: Cardiovascular Imaging*. 2011;4:641–647.
45. Wong YY, Ruiters G, Lubberink M, Raijmakers PG, Knaapen P, Marcus JT, Boonstra A, Lammertsma AA, Westerhof N, Van Der Laarse WJ, Vonk-Noordegraaf A. Right ventricular

failure in idiopathic pulmonary arterial hypertension is associated with inefficient myocardial oxygen utilization. *Circulation: Heart Failure*. 2011;4:700–706.

46. Wong YY, Westerhof N, Ruiters G, Lubberink M, Raijmakers P, Knaapen P, Marcus JT, Boonstra A, Lammertsma AA, Van Der Laarse WJ, Vonk-Noordegraaf A. Systolic pulmonary artery pressure and heart rate are main determinants of oxygen consumption in the right ventricular myocardium of patients with idiopathic pulmonary arterial hypertension. *European Journal of Heart Failure*. 2011;13:1290–1295.
47. Qipshidze N, Tyagi N, Metreveli N, Lominadze D, Tyagi SC. Autophagy mechanism of right ventricular remodeling in murine model of pulmonary artery constriction. *American Journal of Physiology - Heart and Circulatory Physiology*. 2012;302:H688–H696.
48. Mosele F, Tavares AM V, Colombo R, Caron-Lienert R, Araujo ASR, Ribeiro MF, Belló-Klein A. Effects of purple grape juice in the redox-sensitive modulation of right ventricular remodeling in a pulmonary arterial hypertension model. *Journal of Cardiovascular Pharmacology*. 2012;60:15–22.
49. Khoo NKH, Cantu-Medellin N, Devlin JE, St. Croix CM, Watkins SC, Fleming AM, Champion HC, Mason RP, Freeman BA, Kelley EE. Obesity-induced tissue free radical generation: An in vivo immuno-spin trapping study. *Free Radical Biology and Medicine*. 2012;52:2312–2319.
50. Fang Y-H, Piao L, Hong Z, Toth PT, Marsboom G, Bache-Wiig P, Rehman J, Archer SL. Therapeutic inhibition of fatty acid oxidation in right ventricular hypertrophy: Exploiting Randle's cycle. *Journal of Molecular Medicine*. 2012;90:31–43.
51. Fang W, Zhao L, Xiong C-M, Ni X-H, He Z-X, He J-G, Wilkins MR. Comparison of 18F-FDG uptake by right ventricular myocardium in idiopathic pulmonary arterial hypertension and pulmonary arterial hypertension associated with congenital heart disease. *Pulmonary circulation*. 2012;2:365–372.
52. Wong YY, Raijmakers P, Van Campen J, Van Der Laarse WJ, Knaapen P, Lubberink M, Ruiters G, Noordegraaf A V, Lammertsma AA. 11C-acetate clearance as an index of oxygen consumption of the right myocardium in idiopathic pulmonary arterial hypertension: A validation study using 15O-labeled tracers and PET. *Journal of Nuclear Medicine*. 2013;54:1258–1262.
53. Sutendra G, Dromparis P, Paulin R, Zervopoulos S, Haromy A, Nagendran J, Michelakis ED. A metabolic remodeling in right ventricular hypertrophy is associated with decreased angiogenesis and a transition from a compensated to a decompensated state in pulmonary hypertension. *Journal of Molecular Medicine*. 2013;91:1315–1327.
54. Piao L, Fang Y-H, Parikh K, Ryan JJ, Toth PT, Archer SL. Cardiac glutaminolysis: A maladaptive cancer metabolism pathway in the right ventricle in pulmonary hypertension. *Journal of Molecular Medicine*. 2013;91:1185–1197.
55. Drake JJ, Gomez-Arroyo J, Dumur CI, Kraskauskas D, Natarajan R, Bogaard HJ, Fawcett P, Voelkel NF. Chronic carvedilol treatment partially reverses the right ventricular failure transcriptional profile in experimental pulmonary hypertension. *Physiological Genomics*. 2013;45:449–461.

56. Alzoubi A, Toba M, Abe K, O'Neill KD, Rocic P, Fagan KA, McMurtry IF, Oka M. Dehydroepiandrosterone restores right ventricular structure and function in rats with severe pulmonary arterial hypertension. *American Journal of Physiology - Heart and Circulatory Physiology*. 2013;304:H1708–H1718.
57. Piao L, Sidhu VK, Fang YH, Ryan JJ, Parikh KS, Hong Z, Toth PT, Morrow E, Kutty S, Lopaschuk GD, Archer SL. FOXO1-mediated upregulation of pyruvate dehydrogenase kinase-4 (PDK4) decreases glucose oxidation and impairs right ventricular function in pulmonary hypertension: therapeutic benefits of dichloroacetate. *Journal of Molecular Medicine*. 2012;29:1–14.
58. Gomez-Arroyo J, Mizuno S, Szczepanek K, Van Tassell B, Natarajan R, Dos Remedios CG, Drake JJ, Farkas L, Kraskauskas D, Wijesinghe DS, Chalfant CE, Bigbee J, Abbate A, Lesnefsky EJ, Bogaard HJ, et al. Metabolic gene remodeling and mitochondrial dysfunction in failing right ventricular hypertrophy secondary to pulmonary arterial hypertension. *Circulation: Heart Failure*. 2013;6:136–144.
59. Friehs I, Cowan DB, Choi Y-H, Black KM, Barnett R, Del Nido PJ, Levitsky S, McCully JD. Pressure-overload hypertrophy of the developing heart reveals activation of divergent gene and protein pathways in the left and right ventricular myocardium. *FASEB Journal*. 2013;27.
60. Enache I, Charles A-L, Bouitbir J, Favret F, Zoll J, Metzger D, Oswald-Mammosser M, Geny B, Charloux A. Skeletal muscle mitochondrial dysfunction precedes right ventricular impairment in experimental pulmonary hypertension. *Molecular and Cellular Biochemistry*. 2013;373:161–170.
61. Kojonazarov B, Luitel H, Sydykov A, Dahal BK, Paul-Clark MJ, Bonvini S, Reed A, Schermuly RT, Mitchell JA. The peroxisome proliferator-activated receptor beta/delta agonist GW0742 has direct protective effects on right heart hypertrophy. *Pulmonary circulation*. 2013;3:926–935.
62. Yoshinaga K, Ohira H, Tsujino I, Oyama-Manabe N, Mielniczuk L, Beanlands RSB, Katoh C, Kasai K, Manabe O, Sato T, Fujii S, Ito YM, Tomiyama Y, Nishimura M, Tamaki N. Attenuated right ventricular energetics evaluated using 11C-acetate PET in patients with pulmonary hypertension. *European Journal of Nuclear Medicine and Molecular Imaging*. 2014;41:1240–1250.
63. Wang L, Zhang Y, Yan C, He J, Xiong C, Zhao S, Fang W. Evaluation of right ventricular volume and ejection fraction by gated 18F-FDG PET in patients with pulmonary hypertension: Comparison with cardiac MRI and CT. *Journal of Nuclear Cardiology*. 2013;20:242–252.
64. Lundgrin EL, Park MM, Sharp J, Tang WHW, Thomas JD, Asosingh K, Comhair SA, DiFilippo FP, Neumann DR, Davis L, Graham BB, Tudor RM, Dostanic I, Erzurum SC. Fasting 2-deoxy-2-[18F]fluoro-D-glucose positron emission tomography to detect metabolic changes in pulmonary arterial hypertension hearts over 1 year. *Annals of the American Thoracic Society*. 2013;10:1–9.
65. Ikeda S, Satoh K, Kikuchi N, Miyata S, Suzuki K, Omura J, Shimizu T, Fukumoto Y, Sakata Y, Shimokawa H. Crucial role of rho-kinase in pressure-overload-induced right ventricular hypertrophy and dysfunction in mice. *Journal of Cardiac Failure*. 2014;20:S144.
66. Hemnes AR, Brittain EL, Trammell AW, Fessel JP, Austin ED, Penner N, Maynard KB, Gleaves L,

- Talati M, Absi T, Disalvo T, West J. Evidence for right ventricular lipotoxicity in heritable pulmonary arterial hypertension. *Am J Respir Crit Care Med*. 2014;189:325–334.
67. Rawat DK, Alzoubi A, Gupte R, Chettimada S, Watanabe M, Kahn AG, Okada T, McMurtry IF, Gupte SA. Increased reactive oxygen species, metabolic maladaptation, and autophagy contribute to pulmonary arterial hypertension-induced ventricular hypertrophy and diastolic heart failure. *Hypertension*. 2014;64:1266–1274.
  68. Liu B, Luo X-J, Yang Z-B, Zhang J-J, Li T-B, Zhang X-J, Ma Q-L, Zhang G-G, Hu C-P, Peng J. Inhibition of NOX/VPO1 pathway and inflammatory reaction by trimethoxystilbene in prevention of cardiovascular remodeling in hypoxia-induced pulmonary hypertensive rats. *Journal of Cardiovascular Pharmacology*. 2014;63:567–576.
  69. Ahmed LA, Obaid AAZ, Zaki HF, Agha AM. Naringenin adds to the protective effect of l-arginine in monocrotaline-induced pulmonary hypertension in rats: Favorable modulation of oxidative stress, inflammation and nitric oxide. *European Journal of Pharmaceutical Sciences*. 2014;62:161–170.
  70. Frazziano G, Al Ghouleh I, Baust J, Shiva S, Champion HC, Pagano PJ. Nox-derived ROS are acutely activated in pressure overload pulmonary hypertension: Indications for a seminal role for mitochondrial Nox4. *American Journal of Physiology - Heart and Circulatory Physiology*. 2014;306:H197–H205.
  71. Nergui S, Fukumoto Y, Do.e Z, Nakajima S, Shimizu T, Ikeda S, Elias-Al-Mamun M, Shimokawa H. Role of endothelial nitric oxide synthase and collagen metabolism in right ventricular remodeling due to pulmonary hypertension. *Circulation Journal*. 2014;78:1465–1474.
  72. Ahmed LA, Obaid AA, Zaki HF, Agha AM. Role of oxidative stress, inflammation, nitric oxide and transforming growth factor-beta in the protective effect of diosgenin in monocrotaline-induced pulmonary hypertension in rats. *European journal of pharmacology*. 2014;740:379–387.
  73. Zhang W-H, Qiu M-H, Wang X-J, Sun K, Zheng Y, Jing Z-C. Up-regulation of hexokinase1 in the right ventricle of monocrotaline induced pulmonary hypertension. *Respiratory Research*. 2014;15.
  74. Tatebe S, Fukumoto Y, Oikawa-Wakayama M, Sugimura K, Satoh K, Miura Y, Aoki T, Nochioka K, Miura M, Yamamoto S, Tashiro M, Kagaya Y, Shimokawa H. Enhanced [18F]fluorodeoxyglucose accumulation in the right ventricular free wall predicts long-term prognosis of patients with pulmonary hypertension: a preliminary observational study. *European heart journal cardiovascular Imaging*. 2014;15:666–672.
  75. Yang T, Wang L, Xiong C-M, He J-G, Zhang Y, Gu Q, Zhao Z-H, Ni X-H, Fang W, Liu Z-H. The ratio of 18F-FDG activity uptake between the right and left ventricle in patients with pulmonary hypertension correlates with the right ventricular function. *Clinical Nuclear Medicine*. 2014;39:426–430.
  76. Paulin R, Sutendra G, Gurtu V, Dromparis P, Haromy A, Provencher S, Bonnet S, Michelakis ED. A miR-208-Mef2 axis drives the decompensation of right ventricular function in pulmonary hypertension. *Circulation Research*. 2015;116:56–69.

77. Moreira-Gonçalves D, Ferreira R, Fonseca H, Padrão AI, Moreno N, Silva AF, Vasques-Nóvoa F, Gonçalves N, Vieira S, Santos M, Amado F, Duarte JA, Leite-Moreira AF, Henriques-Coelho T. Cardioprotective effects of early and late aerobic exercise training in experimental pulmonary arterial hypertension. *Basic Research in Cardiology*. 2015;110:57.
78. Borgdorff MAJ, Koop AMC, Bloks VW, Dickinson MG, Steendijk P, Sillje HHW, van Wiechen MPH, Berger RMF, Bartelds B. Clinical symptoms of right ventricular failure in experimental chronic pressure load are associated with progressive diastolic dysfunction. *Journal of molecular and cellular cardiology*. 2015;79:244–53.
79. Balestra GM, Mik EG, Eerbeek O, Specht PAC, van der Laarse WJ, Zuurbier CJ. Increased in vivo mitochondrial oxygenation with right ventricular failure induced by pulmonary arterial hypertension: Mitochondrial inhibition as driver of cardiac failure? *Respiratory Research*. 2015;16.
80. Bruns DR, Dale Brown R, Stenmark KR, Buttrick PM, Walker LA. Mitochondrial integrity in a neonatal bovine model of right ventricular dysfunction. *American Journal of Physiology - Lung Cellular and Molecular Physiology*. 2015;308:L158–L167.
81. Kaur G, Singh N, Lingeshwar P, Siddiqui HH, Hanif K. Poly (ADP-ribose) polymerase-1: An emerging target in right ventricle dysfunction associated with pulmonary hypertension. *Pulmonary Pharmacology and Therapeutics*. 2015;30:66–79.
82. Aziz A, Lee AM, Ufere NN, Damiano RJ, Townsend RR, Moon MR. Proteomic Profiling of Early Chronic Pulmonary Hypertension: Evidence for Both Adaptive and Maladaptive Pathology. *Journal of pulmonary & respiratory medicine*. 2015;5.
83. Graham BB, Kumar R, Mickael C, Sanders L, Gebreab L, Huber KM, Perez M, Smith-Jones P, Serkova NJ, Tudor RM. Severe pulmonary hypertension is associated with altered right ventricle metabolic substrate uptake. *American Journal of Physiology - Lung Cellular and Molecular Physiology*. 2015;309:L435–L440.
84. Khan SS, Cuttica MJ, Beussink-Nelson L, Kozyleva A, Sanchez C, Mkrdichian H, Selvaraj S, Dematte JE, Lee DC, Shah SJ. Effects of ranolazine on exercise capacity, right ventricular indices, and hemodynamic characteristics in pulmonary arterial hypertension: a pilot study. *Pulmonary circulation*. 2015;5:547–556.
85. Sakao S, Miyauchi H, Voelkel NF, Sugiura T, Tanabe N, Kobayashi Y, Tatsumi K. Increased right ventricular fatty acid accumulation in chronic thromboembolic pulmonary hypertension. *Annals of the American Thoracic Society*. 2015;12:1465–1472.
86. Li W, Wang L, Xiong C-M, Yang T, Zhang Y, Gu Q, Yang Y, Ni X-H, Liu Z-H, Fang W, He J-G. The Prognostic Value of 18F-FDG Uptake Ratio Between the Right and Left Ventricles in Idiopathic Pulmonary Arterial Hypertension. *Clinical Nuclear Medicine*. 2015;40:859–863.
87. Drozd K, Ahmadi A, Deng Y, Jiang B, Petryk J, Thorn S, Stewart D, Beanlands R, DeKemp RA, DaSilva JN, Mielniczuk LM. Effects of an endothelin receptor antagonist, Macitentan, on right ventricular substrate utilization and function in a Sugen 5416/hypoxia rat model of severe pulmonary arterial hypertension. *Journal of Nuclear Cardiology*. 2016:1–11.

88. Brittain EL, Talati M, Fessel JP, Zhu H, Penner N, Calcutt MW, West JD, Funke M, Lewis GD, Gerszten RE, Hamid R, Pugh ME, Austin ED, Newman JH, Hemnes AR. Fatty acid metabolic defects and right ventricular lipotoxicity in human pulmonary arterial hypertension. *Circulation*. 2016;133:1936–1944.
89. Talati MH, Brittain EL, Fessel JP, Penner N, Atkinson J, Funke M, Grueter C, Jerome WG, Freeman M, Newman JH, West J, Hemnes AR. Mechanisms of Lipid Accumulation in the Bone Morphogenetic Protein Receptor Type 2 Mutant Right Ventricle. *American journal of respiratory and critical care medicine*. 2016;194:719–728.
90. Joshi SR, Dhagia V, Gairhe S, Edwards JG, McMurtry IF, Gupte SA. MicroRNA-140 is elevated and mitofusin-1 is downregulated in the right ventricle of the sugen5416/hypoxia/normoxia model of pulmonary arterial hypertension. *American Journal of Physiology - Heart and Circulatory Physiology*. 2016;311:H689–H698.
91. Peters EL, Offringa C, Kos D, Van der Laarse WJ, Jaspers RT. Regulation of myoglobin in hypertrophied rat cardiomyocytes in experimental pulmonary hypertension. *Pflugers Archiv : European journal of physiology*. 2016;468:1697–1707.
92. Sun X-Q, Zhang R, Zhang H-D, Yuan P, Wang X-J, Zhao Q-H, Wang L, Jiang R, Jan Bogaard H, Jing Z-C. Reversal of right ventricular remodeling by dichloroacetate is related to inhibition of mitochondria-dependent apoptosis. *Hypertension Research*. 2016;39:302–311.
93. Van Der Bruggen CE, Happé CM, Dorfmueller P, Trip P, Spruijt OA, Rol N, Hoevenaars FP, Houweling AC, Girerd B, Marcus JT, Mercier O, Humbert M, Handoko ML, Van Der Velden J, Vonk Noordegraaf A, et al. Bone morphogenetic protein receptor type 2 mutation in pulmonary arterial hypertension: A view on the right ventricle. *Circulation*. 2016;133:1747–1760.
94. Gupte AA, Cordero-Reyes AM, Youker KA, Matsunami RK, Engler DA, Li S, Loebe M, Ashrith G, Torre-Amione G, Hamilton DJ. Differential Mitochondrial Function in Remodeled Right and Nonremodeled Left Ventricles in Pulmonary Hypertension. *Journal of Cardiac Failure*. 2016;22:73–81.
95. Wang L, Li W, Yang Y, Wu W, Cai Q, Ma X, Xiong C, He J, Fang W. Quantitative assessment of right ventricular glucose metabolism in idiopathic pulmonary arterial hypertension patients: A longitudinal study. *European Heart Journal Cardiovascular Imaging*. 2016;17:1161–1168.
96. Sakao S, Daimon M, Voelkel NF, Miyauchi H, Jujo T, Sugiura T, Ishida K, Tanabe N, Kobayashi Y, Tatsumi K. Right ventricular sugars and fats in chronic thromboembolic pulmonary hypertension. *International Journal of Cardiology*. 2016;219:143–149.
97. Ohira H, deKemp R, Pena E, Davies RA, Stewart DJ, Chandy G, Contreras-Dominguez V, Dennie C, Mc Ardle B, Mc Klein R, Renaud JM, DaSilva JN, Pugliese C, Dunne R, Beanlands R, Mielniczuk LM. Shifts in myocardial fatty acid and glucose metabolism in pulmonary arterial hypertension: a potential mechanism for a maladaptive right ventricular response. *European heart journal cardiovascular Imaging*. 2016;17:1424-1431
98. Frille A, Steinhoff KG, Hesse S, Grachtrup S, Wald A, Wirtz H, Sabri O, Seyfarth H-J. Thoracic [18F]fluorodeoxyglucose uptake measured by positron emission tomography/computed

tomography in pulmonary hypertension. *Medicine (United States)*. 2016;95.

99. Campos C, Luz de Castro A, Vicente Tavares AM, Fernandes RO, Ortiz VD, Barboza TE, Pereira C, Apel M, Santos da Silva O, Llesuy S, Sander da Rosa Araujo A, Belló-Klein A. Effect of free and nanoencapsulated copaiba oil on monocrotaline-induced pulmonary arterial hypertension. *Journal of Cardiovascular Pharmacology*. 2017;69:79-85.
100. Liu A, Philip J, Vinnakota KC, Van den Bergh F, Tabima DM, Hacker T, Beard DA, Chesler NC. Estrogen maintains mitochondrial content and function in the right ventricle of rats with pulmonary hypertension. *Physiological Reports*. 2017;5:1-12.
101. He J, Li X, Luo H, Li T, Zhao L, Qi Q, Liu Y, Yu Z. Galectin-3 mediates the pulmonary arterial hypertension-induced right ventricular remodeling through interacting with NADPH oxidase 4. *Journal of the American Society of Hypertension*. 2017;11:275-289.e2.
102. Cowley PM, Wang G, Chang AN, Makwana O, Swigart PM, Lovett DH, Stull JT, Simpson PC, Baker AJ. The alpha1A-adrenergic receptor subtype mediates increased contraction of failing right ventricular myocardium. *American journal of physiology. Heart and circulatory physiology*. 2015;309:H888-96.
103. Tian L, Neuber-Hess M, Mewburn J, Dasgupta A, Dunham-Snary K, Wu D, Chen KH, Hong Z, Sharp WW, Kutty S, Archer SL. Ischemia-induced Drp1 and Fis1-mediated mitochondrial fission and right ventricular dysfunction in pulmonary hypertension. *Journal of Molecular Medicine*. 2017;95:381-393.
104. Nagy BM, Nagaraj C, Egemnazarov B, Kwapiszewska G, Stauber RE, Avian A, Olschewski H, Olschewski A. Lack of ABCG2 leads to biventricular dysfunction and remodeling in response to hypoxia. *Frontiers in Physiology*. 2017;8:1-14.
105. Zhu TT, Zhang WF, Luo P, Qian ZX, Li F, Zhang Z, Hu CP. LOX-1 promotes right ventricular hypertrophy in hypoxia-exposed rats. *Life Sciences*. 2017;174:35-42.
106. Wang X, Shults N V., Suzuki YJ. Oxidative profiling of the failing right heart in rats with pulmonary hypertension. *Plos One*. 2017;12:e0176887.
107. Xu Y, Gu Q, Liu N, Yan Y, Yang X, Hao Y, Qu C. PPAR $\gamma$  alleviates right ventricular failure secondary to pulmonary arterial hypertension in rats. *International Heart Journal*. 2017;58:948-956.
108. dos Santos Lacerda D, Türck P, Gazzi de Lima-Seolin B, Colombo R, Duarte Ortiz V, Poletto Bonetto JH, Campos-Carraro C, Bianchi SE, Belló-Klein A, Linck Bassani V, Sander da Rosa Araujo A. Pterostilbene reduces oxidative stress, prevents hypertrophy and preserves systolic function of right ventricle in cor pulmonale model. *British Journal of Pharmacology*. 2017;174:3302-3314.
109. Puukila S, Fernandes RO, Türck P, Carraro CC, Bonetto JHP, de Lima-Seolin BG, da Rosa Araujo AS, Belló-Klein A, Boreham D, Khaper N. Secoisolariciresinol diglucoside attenuates cardiac hypertrophy and oxidative stress in monocrotaline-induced right heart dysfunction. *Molecular and Cellular Biochemistry*. 2017;432:33-39.

110. Saygin D, Highland KB, Farha S, Park M, Sharp J, Roach EC, Tang WHW, Thomas JD, Erzurum SC, Neumann DR, DiFilippo FP. Metabolic and functional evaluation of the heart and lungs in pulmonary hypertension by gated 2-[18F]-Fluoro-2-deoxy-D-glucose positron emission tomography. *Pulmonary Circulation*. 2017;7:428–438.
111. Siqueira R, Colombo R, Conzatti A, Luz de Castro A, Campos Carraro C, Tavares AMV, Gattelli Fernandes TR, da Rosa Araujo AS, Bello-Klein A. Effects of ovariectomy on antioxidant defence systems in the right ventricle of female rats with pulmonary arterial hypertension induced by monocrotoline. *Canadian Journal of Physiology and Pharmacology*. 2018;96:295–303.